# $^{103}_{46}$Pd$_{57}$

## Evaluation of the decay data

Alan N. Nichols

*Department of Physics, University of Surrey, Guildford GU2 7XH, UK*

Tibor Kibédi

*Department of Nuclear Physics and Accelerator Applications, Australian National University, Canberra, Australia*

The initial evaluation was completed in April 2021 and then successively revised in October 2021, October 2023 and June 2024. The present evaluation was carried out with a literature cut-off date of June 2024.

| $^{103}_{46}$ Pd $_{57}$ |
|---|

## 1 Decay Scheme

$^{103}$Pd disintegrates by almost 100% electron-capture decay via the 39,753-keV metastable state ($^{103m}$Rh) to the ground state of $^{103}$Rh. There is no evidence of an EC transition directly to the ground state of $^{103}$Rh.
*Le $^{103}$Pd se désintègre à presque 100% par capture électronique vers le niveau fondamental du $^{103}$Rh via le niveau excité de 39,753 keV. Aucune transition directe vers le niveau fondamental n'a été observée.*

## 2 Nuclear Data

| | | | | |
|---|---|---|---|---|
| $T_{1/2}$($^{103}$Pd ) | : | 17,00 | (5) | d |
| $T_{1/2}$($^{103m}$Rh ) | : | 56,115 | (16) | min |
| $Q^+$($^{103}$Pd ) | : | 574,7 | (24) | keV |

### 2.1 Electron Capture Transitions

| | Energy (keV) | Probability (%) | Nature | lg $ft$ | $P_K$ | $P_L$ | $P_M$ |
|---|---|---|---|---|---|---|---|
| $\epsilon_{0,5}$ | 37,9 (24) | 0,00480 (16) | allowed | 7,33 | 0,55 (5) | 0,35 (4) | 0,084 (11) |
| $\epsilon_{0,4}$ | 217,3 (24) | 0,0300 (9) | 1st forbidden non-unique | 8,569 | 0,8459 (6) | 0,1226 (4) | 0,02589 (17) |
| $\epsilon_{0,3}$ | 279,7 (24) | 0,00058 (7) | 1st forbidden non-unique | 10,52 | 0,8518 (5) | 0,11804 (26) | 0,02479 (14) |
| $\epsilon_{0,1}$ | 534,9 (24) | 99,9646 (9) | allowed | 5,880 | 0,86086 (30) | 0,11103 (15) | 0,02310 (11) |

## 2.2 Gamma Transitions and Internal Conversion Coefficients

| | Energy (keV) | $P_{\gamma+ce}$ (%) | Multipolarity | $\alpha_K$ | $\alpha_L$ | $\alpha_M$ | $\alpha_T$ |
|---|---|---|---|---|---|---|---|
| $\gamma_{1,0}$(Rh) | 39,753 (6) | 99,9695 (12) | E3+M4 | 142 (7) | 1051 (30) | 214 (6) | 1440 (40) |
| $\gamma_{2,1}$(Rh) | 53,283 (6) | 0,0000190 (12) | (M1) | 1,81 (3) | 0,223 (4) | 0,0415 (6) | 2,08 (3) |
| $\gamma_{4,3}$(Rh) | 62,41 (3) | 0,00282 (10) | M1 | 1,143 (16) | 0,1406 (20) | 0,0262 (4) | 1,314 (19) |
| $\gamma_{5,3}$(Rh) | 241,875 (10) | 0,00000086 (8) | E1 | 0,01033 (15) | 0,001202 (17) | 0,000222 (4) | 0,01179 (17) |
| $\gamma_{3,0}$(Rh) | 294,962 (15) | 0,00340 (11) | M1+E2 | 0,01669 (24) | 0,00199 (3) | 0,000370 (6) | 0,0191 (3) |
| $\gamma_{4,1}$(Rh) | 317,72 (5) | 0,0000175 (17) | E1 | 0,00493 (7) | 0,000571 (8) | 0,0001055 (15) | 0,00563 (8) |
| $\gamma_{4,0}$(Rh) | 357,38 (8) | 0,0271 (8) | E2 | 0,01368 (20) | 0,00181 (3) | 0,000337 (5) | 0,01588 (23) |
| $\gamma_{5,2}$(Rh) | 443,809 (10) | 0,0000189 (12) | E2 | 0,00698 (10) | 0,000889 (13) | 0,0001655 (24) | 0,00807 (12) |
| $\gamma_{5,1}$(Rh) | 497,083 (7) | 0,00477 (16) | M1+E2 | 0,00458 (7) | 0,000539 (8) | 0,0001001 (15) | 0,00524 (8) |

# 3 Atomic Data

## 3.1 Rh

| | | | |
|---|---|---|---|
| $\omega_K$ | : | 0,809 | (4) |
| $\bar{\omega}_L$ | : | 0,0494 | (12) |
| $n_{KL}$ | : | 0,987 | (4) |

### 3.1.1 X Radiations

| | Energy (keV) | Relative probability | |
|---|---|---|---|
| $X_{K_{tot}}$ | 20,073 - 23,173 | 182,8 | |
| $K\alpha_2$ | 20,073 | 52,75 | } $K\alpha$ |
| $K\alpha_1$ | 20,215 | 100 | |
| $K\beta_3$ | 22.699 | 8,51 | } $K'\beta_1$ |
| $K\beta_1$ | 22,725 | 16,56 | |
| KN | 23,167 - 23,173 | 4,96 | |
| $X_{L_{tot}}$ | 2,378 - 3,094 | 21,8 | |
| $X_{M_{tot}}$ | 0,188 - 0,553 | 0,61 | |
| $X_{N_{tot}}$ | 0,029 - 0,063 | 0,0472 | |

### 3.1.2 Auger Electrons

| | Energy (keV) | Relative probability |
|---|---|---|
| Auger $K_{tot}$ | 16,281 - 22,838 | 142,8 |
| KLL | 16,281 - 17,083 | 100 |
| KLX | 19,133 - 20,146 | 39,09 |
| KXY | 21,922 - 22,838 | 3,69 |
| Auger $L_{tot}$ | 0,004 - 3,260 | 1512 |
| Auger $M_{tot}$ | 0,016 – 0,394 | 3985 |
| Auger $N_{tot}$ | 0,001 – 0,058 | 4302 |

## 4 Electron Emissions

| | | Energy (keV) | Electrons (per 100 disint.) |
|---|---|---|---|
| $e_{AN_{tot}}$ | (Rh) | 0,001 - 0,058 | 555 (5) |
| $e_{AM_{tot}}$ | (Rh) | 0,016 - 0,394 | 514 (5) |
| $e_{AL_{tot}}$ | (Rh) | 0,004 - 3,260 | 195,0 (20) |
| $e_{AK_{tot}}$ | (Rh) | 16,281 - 22,838 | 18,42 (9) |
| | KLL | 16,281 - 17,083 | 12,90 (6) |
| | KLX | 19,133 - 20,146 | 5,043 (24) |
| | KXY | 21,922 - 22,838 | 0,4760 (23) |
| $ec_{1,0\ T}$ | (Rh) | 16,533 - 39,751 | 99,9695 (12) |
| $ec_{1,0\ K}$ | (Rh) | 16,533 (6) | 9,9 (6) |
| $ec_{1,0\ L}$ | (Rh) | 36,341 - 36,749 | 73 (3) |
| $ec_{1,0\ M}$ | (Rh) | 39,126 - 39,446 | 14,9 (6) |
| $ec_{1,0\ N}$ | (Rh) | 39,672 - 39,751 | 2,2 (1) |

# 5 Photon Emissions

## 5.1 X-Ray Emissions

| | | Energy (keV) | Photons (per 100 disint.) | |
|---|---|---|---|---|
| $XN_{tot}$ | (Rh) | 0,029 - 0,063 | 0,02001 (14) | |
| $XM_{tot}$ | (Rh) | 0,188 - 0,553 | 0,2595 (23) | |
| $XL_{tot}$ | (Rh) | 2,378 - 3,094 | 9,24 (10) | |
| $XK_{tot}$ | (Rh) | 20,073 - 23,173 | 77,5 (4) | |
| $XK\alpha_2$ | (Rh) | 20,073 | 22,36 (11) | $K\alpha$ |
| $XK\alpha_1$ | (Rh) | 20,215 | 42,39 (20) | |
| $XK\beta_3$ | (Rh) | 22,699 | 3,606 (17) | $K'\beta_1$ |
| $XK\beta_1$ | (Rh) | 22,725 | 7,021 (33) | |
| XKN | (Rh) | 23,167 - 23,173 | 2,104 (10) | |

## 5.2 Gamma Emissions

| | Energy (keV) | Photons (per 100 disint.) |
|---|---|---|
| $\gamma_{1,0}$(Rh) | 39,753 (6) | 0,0694 (19) |
| $\gamma_{2,1}$(Rh) | 53,283 (6) | 0,0000062 (4) |
| $\gamma_{4,3}$(Rh) | 62,41 (3) | 0,00122 (4) |
| $\gamma_{5,3}$(Rh) | 241,875 (10) | 0,00000085 (8) |
| $\gamma_{3,0}$(Rh) | 294,962 (15) | 0,00334 (11) |
| $\gamma_{4,1}$(Rh) | 317,72 (5) | 0,0000174 (17) |
| $\gamma_{4,0}$(Rh) | 357,38 (8) | 0,0267 (8) |
| $\gamma_{5,2}$(Rh) | 443,809 (10) | 0,0000187 (12) |
| $\gamma_{5,1}$(Rh) | 497,083 (7) | 0,00475 (16) |

## 6 Main Production Modes

$^{102}$Pd(n,$\gamma$)$^{103}$Pd

natural-Pd(n,xn)$^{103}$Pd

$^{103}$Rh(p,n)$^{103}$Pd

$^{107}$Ag(p,$\alpha$n)$^{103}$Pd

$^{102}$Pd(d,p)$^{103}$Pd

$^{103}$Rh(d,2n)$^{103}$Pd

$^{107}$Ag(d,$\alpha$2n)$^{103}$Pd

$^{103}$Rh($\alpha$,p3n)$^{103}$Pd

natural-Ag(p,2pxn)$^{103}$Pd

natural-In(p,4pxn)$^{103}$Pd

## 7 References


- A. Flammersfeld. Naturwissenschaften 32 (1944) 36-37
  (Rh-103m half-life)
- M.L. Wiedenbeck. Phys. Rev. 67 (1945) 267-268
  (Rh-103m half-life)
- M.L. Wiedenbeck. Phys. Rev. 68 (1945) 237-239
  (Rh-103m half-life)
- A. Flammersfeld, O. Bruna. Z. Naturforsch. 2a (1947) 241-244
  (Rh-103m half-life)
- D.E. Matthews, M.L. Pool. Phys. Rev. 72 (1947) 163-164
  (Pd-103 half-life)
- M. Lindner, I. Perlman. Phys. Rev. 73 (1948) 1202-1203
  (Pd-103 half-life)
- E. Kondaiah. Phys. Rev. 79 (1950) 891-892
  (40-keV K/(L+M) ratio)
- J.Y. Mei, C.M. Huddleston, A.C.G. Mitchell. Phys. Rev. 79 (1950) 429-432
  (Rh-103m half-life)
- J.M. Cork, J.M. LeBlanc, F.B. Stumpf, W.H. Nestor. Phys. Rev. 86 (1952) 575-576
  (K/L ratios)
- W.W. Meinke. Phys. Rev. 90 (1953) 410-412
  (Pd-103 half-life)
- L.H.Th. Rietjens, H.J. Van Den Bold, P.M. Endt. Physica 20 (1954) 107-114
  (Pd-103 half-life, gamma-ray energies and emission probabilities)
- P. Avignon, A. Michalowicz, R. Bouchez. J. Phys. Radium 16 (1955) 404-410
  (Gamma-ray energies and emission probabilities, ICC(K), ICC(L), K/L ratio)
- G.M. Drabkin, V.I. Orlov, L.I. Rusinov. Izv. Akad. Nauk SSSR, Ser. Fiz., Columbia Tech. Transl. 19 (1955) 294-304
  (ICC(K), K/L ratio, L/M ratio)
- F.K. McGowan, P.H. Stelson. Phys. Rev. 99 (1955) 127-134
  (Mixing ratio (295 keV))
- B. Saraf. Phys. Rev. 97 (1955) 715-720
  (Gamma-ray energies and emission probabilities)
- G.A. Jones, W.R. Phillips. Proc. Royal Soc. (London) 239A (1957) 487-493
  (Rh-103m half-life)
- F.K. McGowan, P.H. Stelson. Phys. Rev. 109 (1958) 901-916
  (Mixing ratio (295 keV))
- A.M. Bresesti, M. Bresesti, H. Neumann. J. Inorg. Nucl. Chem. 29 (1967) 15-20
  (Ru-103 beta decay: K X-ray emission probabilities, K/(L+M+N) ratio (39.75 keV))

- A. Vuorinen. Proc. Symp. Standardization of Radionuclides, IAEA, Vienna, Austria (1967)
  (Rh-103m half-life, K/(K+L+M) ratio, K X-ray emission probabilities (39.75 keV))
- R.S. Hager, E.C. Seltzer. Nucl. Data A4 (1968) 1-235
  (Theoretical ICC)
- J.C. Manthuruthil, H.J. Hennecke, C.R. Cothern. Phys. Rev. 165 (1968) 1363-1370
  (ICC, multipolarities, mixing ratios)
- J.A. Panontin, N.T. Porile, A.A. Caretto Jr. Phys. Rev. 165 (1968) 1273-1281
  (Pd-103 half-life)
- Y. Grunditz, S. Antman, H. Pettersson, M. Saraceno. Nucl. Phys. A133 (1969) 369-384
  (Pd-103 half-life, gamma-ray energies and emission probabilities, ICC(K), subshell ratios, K X-ray emission probabilities, (P(357 keV)/P(K X-ray)))
- Y. Kobayashi. JAERI report JAERI-1178 (1969) 21-22
  (Rh-103m half-life)
- M.A. Lepri, W.S. Lyon. Int. J. Appl. Radiat. Isot. 20 (1969) 297-298
  (K(alpha)/K(beta), 39.75-keV ICC(K))
- D.E. Raeside, J.J. Reidy, M.L. Wiedenbeck. Nucl. Phys. A134 (1969) 347-352
  (Gamma-ray energies, ICC(K))
- W.H. Zoller, E.S. Macias, M.B. Perkal, W.B. Walters. Nucl. Phys. A130 (1969) 293-304
  (Gamma-ray energies and emission probabilities, 497-keV ICC(K), gamma-gamma coincidence)
- E.B. Nieschmidt, D.A. Pearson. IN-1317 (1970) 122-126
  (Gamma-ray energies and emission probabilities, ICC(K), L subshell ratios)
- H. Pettersson, S. Antman, Y. Grunditz. Z. Phys. 233 (1970) 260-274
  (Gamma-ray energies, L1/L2, L1/L3, L2/L3 ratios, ICC(K))
- H. Pettersson, S. Antman, Y. Grunditz. Erratum, Z. Phys. 235 (1970) 485
  (ICC(K))
- W.M. Roney, H.W. Kugel, G.M. Heestand, R.R. Borchers, R. Kalish. Proc. Int. Conf. Nuclear Reactions Induced by Heavy Ions, 15-18 July 1969, Heidelberg, Germany (1970) 419-423
  (Mixing ratio (295 keV))
- F.T. Avignone III, G.D. Frey. Phys. Rev. C 4 (1971) 912-918
  (ICC(K), K/(L+M+ ...) ratio, multipolarity)
- W. Bambynek, B. Crasemann, R.W. Fink, H.-U. Freund, H. Mark, C.D. Swift, R.E. Price, P. Venugopala Rao. Rev. Mod. Phys. 44 (1972) 716-813
  (K-shell fluorescence yield)
- D.S. Brenner, M.L. Perlman. Nucl. Phys. A181 (1972) 207-216
  (39.75-keV L1/L3, L2/L3 ratios)
- H.C. Jain, S.K. Bhattacherjee, C.V.K. Baba. Nucl. Phys. A178 (1972) 437-448
  (Half-life of 93-keV nuclear level of Rh-103)
- A. Pazsit, J. Csikai. Sov. J. Nucl. Phys. 35 (1972) 232-233
  (Rh-103m half-life, 39.75-keV ICC(K))
- R.O. Sayer, J.K. Temperley, D. Eccleshell. Nucl. Phys. A179 (1972) 122-140
  (Mixing ratio (295 keV))
- Chr. Bargholtz, J. Becker, L. Eriksson, L. Gidefeldt, L. Holmberg, V. Stefansson. Physica Scripta 8 (1973) 90-94
  (Half-life of 93-keV nuclear level of Rh-103)
- E. Günther, K. Knauf, K.F. Walz. Int. J. Appl. Radiat. Isot. 24 (1973) 87-89
  (Rh-103m half-life)
- H. Ing, W.G. Cross. Int. J. Appl. Radiat. Isot. 24 (1973) 437-450
  (Ru-103 beta decay: K X-ray emission probabilities)
- W. Bambynek, B. Crasemann, R.W. Fink, H.-U. Freund, H. Mark, C.D. Swift, R.E. Price, P. Venugopala Rao. Erratum, Rev. Mod. Phys. 46 (1974) 853
  (K-shell fluorescence yield)
- K.H. Czock, N. Haselberger, F. Reichel. IAEA report IAEA/RL/26 (1974)
  (ICC(total), ICC(K), K/(L+M+ N) ratio)
- D.C. Santry, J.P. Butler. Can. J. Phys. 52 (1974) 1421-1428
  (Rh-103m half-life, K X-ray emission probabilities)
- K.H. Czock, N. Haselberger, F. Reichel. Int. J. Appl. Radiat. Isot. 26 (1975) 417-421
  (ICC(total), ICC(K), K X-ray emission probabilities)
- K.H. Czock, N. Haselberger, F. Reichel, S. Popa. Int. J. Appl. Radiat. Isot. 26 (1975) 782-784
  (Pd-103 half-life)

- B. Martin, D. Merkert, J.L. Campbell. Z. Phys. A274 (1975) 15-21
  (39.75-keV L1/L2, L1/L3, L2/L3, M, N, O ratios)
- E.S. Macias, M.E. Phelps, D.G. Sarantites, R.A. Meyer. Phys. Rev. C 14 (1976) 639-644
  (Gamma-ray energies and emission probabilities, ICC(K), ICC(L), K X-ray emission probabilities, (P(357 keV)/P(K X-ray)) ratio)
- K.S. Krane. At. Data Nucl. Data Tables 19 (1977) 363-416
  (Mixing ratios)
- F.P Larkins. At. Data Nucl. Data Tables 20 (1977) 311-387
  (Auger-electron energies)
- F. Lagoutine, J. Legrand, C. Bac. Int. J. Appl. Radiat. Isot. 29 (1978) 269-272
  (Rh-103m half-life)
- D. Newton, A.E.R. Toureau, A.L. Anderson, R.A. Meyer. Int. J. Appl. Radiat. Isot. 29 (1978) 188-189
  (Gamma-ray energies and emission probabilities, (P(375 keV)/P(K X-ray)) ratio)
- R. Vaninbroukx, G. Grosse, W. Zehner. NEA report NEANDC(E)-202U Vol. III (1979) 28-30
  (Rh-103m gamma-ray emission probability, K X-ray emission probabilities, ICC(total), ICC(K))
- E. Hagn, J. Wese, G. Eska. Z. Phys. - Atoms and Nuclei A299 (1981) 353-358
  (Mixing ratio (497.1 keV))
- D.W. Murray, A.L. Allsop, N.J. Stone. Hyperfine Interactions 11 (1981) 127-139
  (Mixing ratio (497.2 keV))
- R. Vaninbroukx, G. Grosse, W. Zehner. Int. J. Appl. Radiat. Isot. 32 (1981) 589-591
  (Pd-103 and Rh-103m half-lives)
- R. Vaninbroukx, W. Zehner. Int. J. Appl. Radiat. Isot. 32 (1981) 850
  (Rh-103m K X-ray emission probabilities)
- K.S. Krane. Phys. Rev. C 27 (1983) 411-412
  (Mixing ratio (497.1keV))
- S.T. Perkins, D.E. Cullen, M.H. Chen, J.H. Hubbell, J. Rathkopf, J. Scofield. Lawrence Livermore National Laboratory report UCRL-50400 30 (1991)
  (Atomic database)
- D.E. Cullen, S.T. Perkins, S.M. Seltzer. Appl. Radiat. Isot. 44 (1993) 1343-1347
  (Atomic database)
- U. Schötzig. Appl. Radiat. Isot. 45 (1994) 641-644
  (K X-ray emission probabilities)ö
- E. Schönfeld. PTB report PTB-6.33-95-2 (1995)
  (P(K), P(L), P(M), P(N), P(O))
- E. Schönfeld, H. Janssen. Nucl. Instrum. Methods Phys. Res. A369 (1996) 527-533
  (K-, L-shell fluorescence yields, K(beta)/K(alpha), K(alpha2)/K(alpha1), KLX/KLL, KXY/KLL)
- E. Schönfeld, G. Rodloff. PTB report PTB-6.11-98-1 (1998)
  (Auger electrons)
- E. Schönfeld. Appl. Radiat. Isot. 49 (1998) 1353-1357
  (P(K), P(L), P(M), P(N), P(O))
- M. Sainath, K. Venkataramaniah. Indian J. Pure Appl. Phys. 37 (1999) 87-91
  (ICC(K), ICC(L), ICC(M) 39.75 keV)
- E. Schönfeld, G. Rodloff. PRB report PTB-6.11-1999-1 (1999)
  (X(K))
- A. Kovalik, A.F. Novgorodov, E.A. Yakushev, V.M. Gorozhankin, P. Petev, M.A. Mahmoud. Proc. 50th Ann. Conf. Nucl. Spectrosc. Struct. At. Nuclei, St. Petersburg, Russia (2000) 176
  (Rh-103m KLL Auger spectrum)
- A. Kovalik, E.A. Yakushev, D.V. Filosofov, V.M. Gorozhankin, V.G. Kalinnikov. Proc. 50th Ann. Conf. Nucl. Spectrosc. Struct. At. Nuclei, St. Petersburg, Russia (2000) 175
  (39.7537(21)-keV gamma-ray energy)
- A. Kovalik, E.A. Yakushev, D.V. Filosofov, A.F. Novgorodov, V.M. Gorozhankin, I. Stekl, P. Petev, M.A. Mahmoud. Proc. 50th Ann. Conf. Nucl. Spectrosc. Struct. At. Nuclei, St. Petersburg, Russia (2000) 178
  (Rh-103m KL1L2 Auger spectrum)
- E. Schönfeld, H. Janssen. Appl. Radiat. Isot. 52 (2000) 595-600
  (X-ray emission probabilities, Auger-electron emission probabilities)
- D. De Frenne, E. Jacobs. Nucl. Data Sheets 93 (2001) 447-598
  (Nuclear levels)
- I.M. Band, M.B. Trzhaskovskaya, C.W. Nestor Jr., P.O Tikkanen, S. Raman. At. Data Nucl. Data Tables 81 (2002) 1-334
  (Theoretical ICC)

- S. Raman, C.W. Nestor Jr., A. Ichihara, M.B. Trzhaskovskaya. Phys. Rev. C 66 (2002) 044312
  (Theoretical ICC)
- T.P. Berlyand, E.I. Grigor'ev, V.P. Orlov. Measurement Techniques 45 (2002) 974-977
  (Gamma-ray emission probabilities, X-ray emission probabilities, K(alpha)/K(beta), (P(357 keV)/P(K X-ray)))
- Yu.S. Popov, L.V. Zakharova, V.N. Kupriyanov, O.I. Andreev, A.N. Pakhomov, F.Z. Vakhetov. Radiochemistry 46 (2004) 209-210
  (Pd-103 half-life, gamma-ray emission probabilities, X-ray emission probabilities, K(alpha)/K(beta))
- T. Kibédi, T.W. Burrows, M.B. Trzhaskovskaya, P.M. Davidson, C.W. Nestor Jr. Nucl. Instrum. Methods Phys. Res. A589 (2008) 202-229
  (Theoretical ICC)
- D. De Frenne. Nucl. Data Sheets 110 (2009) 2081-2256
  (Nuclear levels)
- F. Tarkanyi, A. Hermanne, B. Kiraly, S. Takacs, F. Ditroi, J. Csikai, A. Fenyyesi, M.S. Uddin, M. Hagiwara, M. Baba, T. Ido, Yu.N. Shubin, A.V. Ignatyuk. Appl. Radiat. Isot. 67 (2009) 1574-1581
  (Discrepancies in gamma-ray and K X-ray emission probabilities)
- K.S. Krane. Phys. Rev. C 81 (2010) 044310
  (Gamma-ray energies, Rh-103 nuclear level energies)
- B.Q. Lee, T. Kibédi, A.E. Stuchbery, K.A. Robertson. Compt. Math. Methods Med. Article ID 651475 (2012) 1-14
  (Atomic radiation)
- B.Q. Lee, T. Kibédi, A.E. Stuchbery, K.A. Robertson, F.G. Kondev. Proc. Heavy Ion Accelerator Symposium (HIAS2013), 8-12 April 2013, Canberra, Australia, EPJ Web of Conferences 63 (2013) 01002
  (Auger electrons)
- X. Mougeot. Erratum, Phys. Rev. C 92 (2015) 059902
  (Beta decay, BetaShape code)
- X. Mougeot. Phys. Rev. C 91 (2015) 055504
  (Beta decay, BetaShape code)
- B.Q. Lee, Hooshang Nikjoo, J. Ekman, P. Jonsson, A.E. Stuchbery, T. Kibédi. Int. J. Radiat. Biol. 92 (2016) 641-653
  (Atomic radiation)
- N. Nica, J.C. Hardy, V.E. Iacob, V. Horvat, H.I. Park, T.A. Werke, K.J. Glennon, C.M. Folden III, V.I. Sabla, J.B. Bryant, X.K. James, M.B. Trzhaskovskaya. Phys. Rev. C 98 (2018) 054321
  (ICC(K), ICC(total), mixing ratio 39.75 keV)
- J. Riffaud, P. Cassette, D. Lacour, V. Lourenco, I. Tartès, M.A. Kellett, M. Corbel, M.-C. Lépy, C. Domergue, C. Destouches, H. Carcreff, O. Vigneau. Appl. Radiat. Isot. 134 (2018) 399-405
  (Rh-103m IT decay: absolute K X-ray emission probabilities, absolute gamma-ray emission probability)
- X. Mougeot. Appl. Radiat. Isot. 154 (2019) 108884
  (EC/positron decay, BetaShape code)
- B.P.E. Tee, T. Kibédi, B.Q. Lee, M. Vos, R. du Rietz, A.E. Stuchbery. Proc. Heavy Ion Accelerator Symposium (HIAS2019), 9-13 September 2019, Canberra, Australia, EPJ Web of Conferences 232 (2020) 01006
  (Atomic radiation)
- F.G. Kondev, Meng Wang, W.J. Huang, S. Naimi, G. Audi. Chin. Phys. C 45 (2021) 030001
  (Rh-103m Q(IT))
- Meng Wang, W.J. Huang, F.G. Kondev, G. Audi, S. Naimi. Chin. Phys. C 45 (2021) 030003
  (Q-values)
- J. Riffaud, M.-C. Lépy, P. Cassette, M. Corbel, M.A. Kellett, V. Lourenco. Appl. Radiat. Isot. 167 (2021) 109298
  (Pd-103 half-life, absolute K X-ray emission probabilities, relative L X-ray emission probabilities, absolute gamma-ray emission probabilities)
- X. Mougeot. Appl. Radiat. Isot. 201 (2023) 111018
  (Beta decay, BetaShape code)
- B.P.E. Tee, T. Kibédi, B.Q. Lee, A.E. Stuchbery. BrIccEmisDB database, in preparation for submission to At. Data Nucl. Data Tables (2023)
  (Atomic radiation)

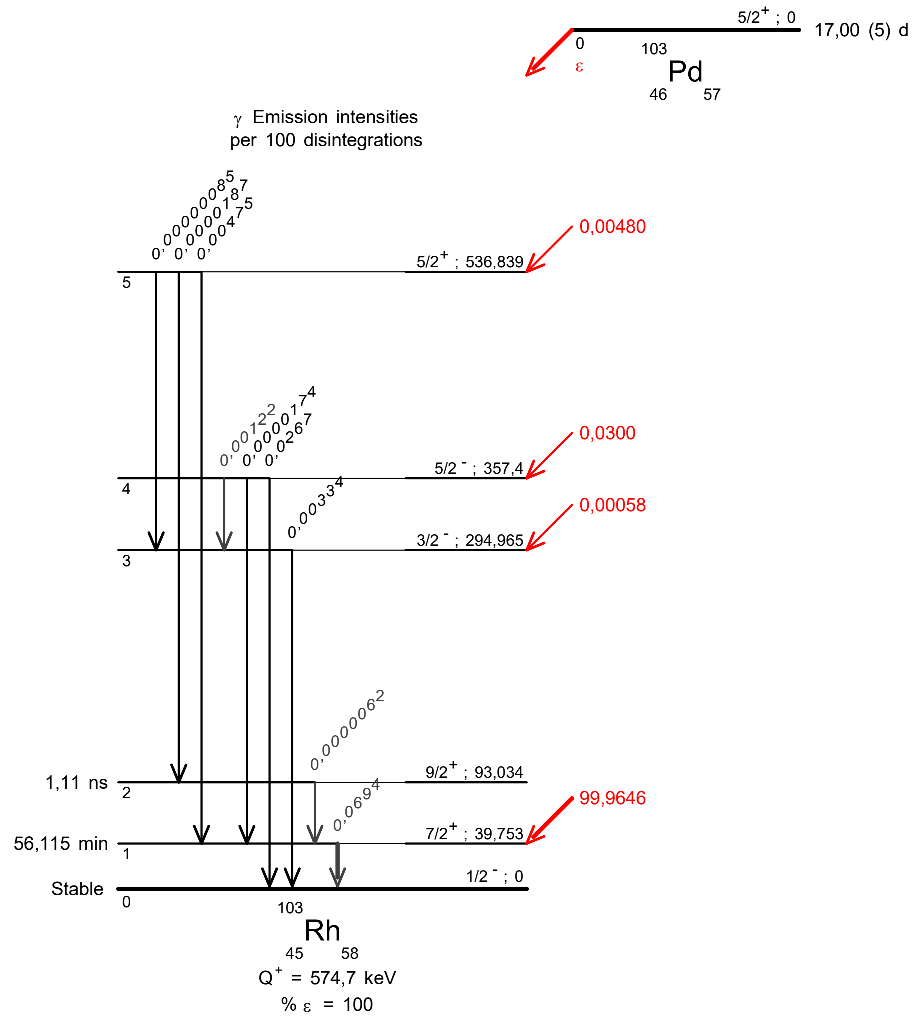
5/2+ ; 0
17,00 (5) d
0
ε
103 Pd 46 57
γ Emission intensities
per 100 disintegrations
0,00000855
0,0000187
0,000475
5/2+ ; 536,839
0,00480
5
0,00122
0,000174
0,000267
5/2 - ; 357,4
0,0300
4
0,00334
3/2 - ; 294,965
0,00058
3
0,0000062
1,11 ns
2
9/2+ ; 93,034
0,0694
99,9646
56,115 min
1
7/2+ ; 39,753
Stable
0
1/2 - ; 0
103 Rh 45 58
Q+ = 574,7 keV
% ε = 100

# $^{103}$Pd/$^{103m}$Rh – Comments on evaluation of decay data by A. L. Nichols[1], T. Kibédi[2]

[1] Department of Physics, University of Surrey, Guildford GU2 7XH, UK
[2] Department of Nuclear Physics, The Australian National University (ANU), Canberra ACT, Australia

**Reviewer: S. Leblond**

Université Paris-Saclay, CEA, Laboratoire National Henri Becquerel (LNE-LNHB), 91120 Palaiseau, France

**Evaluated: March/April 2021, September/October 2021, October 2023, June 2024**

## Evaluation Procedures

*Limitation of Relative Statistical Weight Method* (LWM) and other analytical techniques were applied to average numbers throughout the evaluation. The uncertainty assigned to the average value was always greater than or equal to the smallest uncertainty of the values used to calculate the average.

### Decay Scheme

$^{103}$Pd ($T_{½}$ = 17.00 days) decays almost 100% by electron capture decay ($Q_{EC}$ = 534.9 (24) keV) to the metastable excited state of $^{103m}$Rh to be followed by IT decay ($T_{½}$ = 56.115 minutes) to the ground state of $^{103}$Rh ($Q_{IT}$ = 39.753 (6) keV), as quantified in 2021Wa16 and 2021Ko07. While the full EC decay process consists of four EC transitions and nine gamma-ray emissions to the ground state of $^{103}$Rh, the decay scheme is dominated by EC decay directly to the 39.753-keV excited state of $^{103m}$Rh and the resulting IT gamma transition to the stable $^{103}$Rh ground state. However, a number of difficulties arise as a consequence of the lack of significant agreement between the X-ray and gamma-ray measurements of 1969Zo02, 1969Gr13, 1970NiZV, 1976Ma37, 2002Bf07, 2004Po24, 2018Ri01 and 2021Ri01 (particularly the important relative emission probability of the 39.753-keV gamma ray). Under these rather difficult circumstances, the decision was taken to assess the weighted-mean relative emission probabilities of the gamma-ray studies by 1976Ma37 and 2021Ri01 on the basis of their reported accuracy, consistency and completeness, along with consideration of data subsets selected from the measurements of 1969Zo02, 2002Bf07 and 2004Po24. All relative gamma-ray emission probabilities were defined in terms of the 357.42-keV gamma ray (100).

### Nuclear Data

There is a strong interest in the well-defined nuclear levels of $^{103}$Rh populated in the EC decay of $^{103}$Pd because of the adoption of this monoisotopic element ($^{103}$Rh) as a neutron flux monitor. $^{103}$Pd decay is also viewed as a suitable electron and X-ray emitter for microdosimetry and radiotherapy in nuclear medicine.

## Half-life of $^{103}$Pd

The measurements of 1953Me24, 1975Cz05, 1981Va11 and 2021Ri01were adopted to give a weighted mean half-life of 17.00 (5) days based on the LWM analytical technique (Avetools code, version 3.0, and V.AveLib 06-22 code, both ENSDF utility programs).

| Reference | Half-life (d) | Selected detail, issues and uncertainties |
|---|---|---|
| 1947Ma32 | 17.0 | no uncertainty quoted – not adopted in analytical procedures |
| 1948Li03 | 17 | no uncertainty quoted – not adopted in analytical procedures |
| **1953Me24** | **17.0 ± 0.4** | long-lived component after neutron irradiation of Pd target (Geiger-Muller tube: activity followed over 60 d) |
| 1954Ri09 | 17.5 ± 0.5 | X rays, total γ spectrum, 60- to 250-, 367- and 503-keV γ rays (NaI(Tl) crystal over 15 d (reference Fig. 2)); outlier (Chauvenet criterion) – not adopted in analytical procedures |
| 1968Pa24 | 16.9 ± 0.1 | sparse information - analysis of X-ray decay curves from proton-irradiated silver and indium targets (NaI(Tl) crystal over unspecified times) – not adopted in analytical procedures |
| 1969Gr13 | 18.4 ± 0.5 | conversion/Auger electrons, KX rays and γ rays (double-focussing β spectrometer and Ge(Li) detector over 70 d); significant outlier (Chauvenet criterion) – not adopted in analytical procedures |
| **1975Cz05** | **16.961 ± 0.016[a]** | conversion/Auger electrons (4π-proportional flow counter over 80 d) and 20-keV KX rays (NaI(Tl) crystal and Ge(Li) detector over 32 and 36 d, respectively) – focus on Ge(Li) data |
| **1981Va11** | **16.991 ± 0.019[b]** | decay of KX rays (Si(Li) detectors) and γ rays (NaI(Tl) crystal over 33 to 54 d); detailed definition of systematic uncertainties |
| 2004Po24 | 16.8 ± 0.6 | decay of 295-, 358- and 479-keV γ rays over ~ 100 d by means of HPGe detector; outlier – not adopted in final analytical procedure |
| **2021Ri01** | **17.049 ± 0.016** | regular determination of peak area of 357.4-keV γ ray over 50 d by means of HPGe detector; well-defined uncertainties |
| **Recommended value** | **17.00 ± 0.05** | **LWM, with uncertainty expanded from ± 0.03 to ± 0.05 to cover 17.049 ± 0.016 of 2021Ri01; $\chi^2/(N-1)$ of 5.18 and $\chi^2/(N-1)_{critical}$ at 99% confidence level of 3.78 after a second pass; UWM of 17.000 ± 0.018** |

[a] Weighted mean of three sets of measurements is 16.953 (7), compared with an adopted value of 16.961 (16) quoted by 1975Cz05.
[b] Weighted mean of four sets of measurements is 16.992 (10), compared with an adopted value of 16.991 (19) quoted by 1981Va11.

Consideration was given to the unweighted mean (UWM), limitation of relative statistical weight method (LWM), normalised residual method (NRM), Rajeval technique, expected value method (EVM), bootstrap method and Mandel-Paule approach in analyses of the data set.

| Analytical method | Half-life (d) | $\chi^2/(N-1)$ | $\chi^2/(N-1)_{critical}$ |
|---|---|---|---|
| UWM | 17.00 ± 0.10 | – | – |
| LWM | 17.00 ± 0.03 | 5.18 | 2.60 for rejection at 95% confidence level |
| NRM | 16.984 ± 0.017 | 2.19 | 2.60 for rejection at 95% confidence level |
| Rajeval | 16.990 ± 0.016 | 0.69 | 2.60 for rejection at 95% confidence level |
| EVM | 17.00 ± 0.08 | – | 89.3% confidence level |
| Bootstrap | 17.00 ± 0.06 | 5.19 | – |
| Mandel-Paule | 17.001 ± 0.033 | 5.18 | – |

Although a number of difficulties arose during the course of this exercise, a half-life value of (17.00 ± 0.05) days was derived and recommended for $^{103}$Pd, as quantified by the LWM analytical procedure. However, these studies demonstrated the requirement for further accurate measurements of this decay parameter.

## Half-life of daughter $^{103m}$Rh

The measurements of 1967VuZZ, 1969KoZW, 1973Gu06, 1974Sa15, 1978La21 and 1981Va11 were adopted to give a weighted mean half-life of 56.115 (16) min based on the LWM-NRM-Rajeval analytical techniques.

| Reference | Half-life (min) | Selected detail, issues and uncertainties |
|---|---|---|
| 1944Fl01 | 48 ± 5 | $^{103}$Rh(n$_f$,n') reaction – outlier (Chauvenet criterion), and therefore not included in analytical procedures |
| 1945Wi03/1945Wi12 | 45 ± 1 | $^{103}$Rh(X,γ) reaction – outlier (Chauvenet criterion), and therefore not included in analytical procedures |
| 1947Fl03 | 52 ± 2 | $^{103}$Rh(d,d') reaction – outlier (Chauvenet criterion), and therefore not included in analytical procedures |
| 1950Me26 | 56 | separation of Pd target and $^{103m}$Rh – uncertainty not specified, and therefore not included in analytical procedures |
| 1957Jo19 | 57.5 ± 0.5 | $^{103}$Rh(n,n') reaction – outlier (Chauvenet criterion), and therefore not included in analytical procedures |
| 1967VuZZ | **56.6 ± 0.4** | $^{103}$Rh(n,n') reaction; 4π proportional counter and thin NaI crystal |
| 1969KoZW | **56.6 ± 0.6** | $^{102}$Ru(n,γ)$^{103}$Ru(β$^-$)$^{103m}$Rh; radiochemical separation, NaI(Tl) scintillation counter |
| 1972Pa10 | 57.5 | $^{103}$Rh(n$_{14.7keV}$,n') reaction, Si(Li) detector – uncertainty not specified, and therefore not included in analytical procedures |
| 1973Gu06 | **56.116 ± 0.009** | $^{nat}$Pd(n,xn')$^{103}$Pd(EC)$^{103m}$Rh; three counting techniques: liquid scintillation counter, 2π-methane flow counter, and NaI(Tl) crystal – weighted mean of three sets of measurements is 56.116 (7), compared with a value of 56.116 (9) quoted by 1973Gu06; uncertainty adjusted to ± 0.016 to reduce weighting to ~ 0.50 |
| 1974Sa15 | **56.3 ± 0.6** | $^{103}$Rh(n,n') reaction; decay curve followed over many half-lives, NaI(Tl) X-ray detector |
| 1978La21 | **56.112 ± 0.028** | ion exchange of $^{103m}$Rh from $^{103}$Pd solutions; decay curves involving 15 sources followed over three half-lives by means of an ill-defined photon spectrometer |
| 1979VaZE | 56.1 ± 0.1 | preliminary measurement - replaced by half-life determined by 1981Va11 |
| 1981Va11 | **56.114 ± 0.020** | ion exchange of $^{103m}$Rh from $^{103}$Pd solutions; decay curves followed over two and three half-lives, NaI(Tl) detector – weighted mean of two sets of measurements is 56.114 (12), compared with a value of 56.114 (20) quoted by 1981Va11 |
| **Recommended value** | **56.115 ± 0.016** | recommended uncertainty adjusted from ± 0.011 to ± 0.016, to align with smallest uncertainty of the values used to calculate weighted-mean value |

Limitation of relative statistical weight method (LWM), normalized residual method (NRM), Rajeval technique, expected value method (EVM), bootstrap method and Mandel-Paule approach were considered in the analysis of the data set.

| Analytical method | Half-life (min) | $\chi^2/(N-1)$ | $\chi^2/(N-1)_{critical}$ |
|---|---|---|---|
| UWM | 56.31 ± 0.16 | – | – |
| LWM | 56.115 ± 0.011 | 0.45 | 2.21 for rejection of 95.0% confidence level |
| NRM | 56.115 ± 0.011 | 0.45 | 2.21 for rejection at 95.0% confidence level |
| Rajeval | 56.115 ± 0.011 | 0.45 | 2.21 for rejection at 95.0% confidence level |
| EVM | 56.13 ± 0.08 | – | 97.0% confidence level |
| Bootstrap | 56.22 ± 0.16 | 15.8 | – |
| Mandel-Paule | 56.115 ± 0.011 | 0.45 | – |

Half-life of (56.115 ± 0.016) minutes was recommended for $^{103m}$Rh, as quantified by the LWM-NRM analytical procedures (with 1973Gu06 uncertainty increased to ± 0.016 in order to adjust weighting to ~ 0.50).

## $^{103}$Pd/$^{103m}$Rh parent-daughter equilibrium

## Q values

A $Q_{EC}$ value for $^{103}$Pd EC decay of 534.9 (24) keV to the excited metastable state of $^{103m}$Rh and subsequent

IT decay with $Q_{IT}$ of 39.753 (6) keV to the ground state of $^{103}$Rh have been adopted (2021Ko07, 2021Wa16), to give a $Q_{EC}$ value of 574.7 (24) keV for $^{103}$Pd EC decay to the stable ground state of $^{103}$Rh.

## Gamma-ray energies and emission probabilities

Energies

The energies of the gamma-ray emissions have been reasonably well measured by 1969Zo02, 1969Gr13, 1969Ra18, 1970NiZV, 1970Pe04, 1976Ma37 and 2010Kr05, and therefore individual weighted-mean values were determined from these data. GTOL version 7.2h (24-May-2013) is an ENSDF analysis code that was used to undertake least-squares fits to the evaluated gamma-ray energies, and re-define the energies of the proposed nuclear levels of $^{103}$Rh for comparison with the equivalent level energies recommended by 2009De29. Nuclear-level energies were subsequently determined in this manner, except for the highly-converted (E3 + M4) 39.753-keV gamma transition and associated nuclear level which were preferably identified with a gamma transition energy of 39.7537 (21) keV as determined from $K_{ce}$ and the K-shell electron binding energy (2000KoZT), and also in exact alignment with a $Q_{IT}$ of 39.753 (6) keV adopted in NUBASE2020 (2021Ko07, 2021Wa16).

**Adopted energies, spins and parities for the nuclear levels of $^{103}$Rh (GTOL v7.2h and 2009De29).**

| Nuclear level number | Nuclear level energy (keV) | | Spin and parity | Half-life |
|---|---|---|---|---|
| | GTOL v7.2h | 2009De29 | | |
| 0 | 0.0 | 0.0 | 1/2 $^-$ | stable |
| 1 | 39.752 ± 0.006 | **39.753 ± 0.006** | 7/2 $^+$ | (56.115 ± 0.016) min. |
| 2 | **93.034 ± 0.008** | 93.036 ± 0.009 | 9/2 $^+$ | (1.11 ± 0.03) ns [a] |
| 3 | **294.965 ± 0.010** | 294.965 ± 0.008 | 3/2 $^-$ | |
| 4 | **357.40 ± 0.03** | 357.396 ± 0.017 | 5/2 $^-$ | |
| 5 | **536.839 ± 0.008** | 536.840 ± 0.007 | 5/2 $^+$ | |

[a] Weighted-mean value of 1.114 (24) ns determined from measurements of 1.13 (3) ns by plastic scintillator and 1.13 (7) ns by beta spectrometer (1972Ja01) and 1.06 (5) ns by delayed coincidence with NaI(Tl) detector and plastic scintillator (1973Ba52); uncertainty increased from ± 0.024 to ± 0.03 ns in alignment with the smallest uncertainty of the values used to calculate the weighted mean.

Emission Probabilities

Relative gamma-ray emission probabilities have been partially or fully determined in the measurements of 1969Zo02, 1969Gr13, 1970NiZV, 1976Ma37, 2002Bf07, 2004Po24 and 2021Ri01 by means of various numbers/arrays and types of high-resolution Ge(Li) detector and HPGe (significantly earlier studies of 1954Ri09, 1955Av11 and 1955Sa16 involved the use of NaI(Tl) scintillators). Unfortunately, specific subsets of the more recent individual datasets are judged as being disparate – relative gamma-ray emission probabilities normalised to $P_{\gamma}$(357.38 keV) of 100 differ widely by a factor of 1.2 to 2.0 for the prominent 39.753- and 62.41-keV gamma-ray emissions as measured by 1976Ma37 and 2021Ri01 when compared with the equivalent measurements of 1969Zo02 and 1970NiZV, while more modest disagreement is found to within a factor of between 0.7 to 0.8 for the higher-energy 62.4-, 295- and 497-keV gamma rays. There are also similar modest disagreements between 1976Ma37/2021Ri01 and 1969Gr13 for the 62.4-, 295- and 497-keV gamma rays, although the relative gamma-ray emission probability of the dominant 39.753-keV gamma ray as measured by 1969Gr13 is a significant factor of 2.6/2.2 smaller than that determined by 1976Ma37/2021Ri01. Under these rather difficult circumstances, the decision was taken to favour overall the measurements of Macias *et al*. (1976Ma37) and Riffaud *et al.* (2021Ri01) on the basis of their reported accuracy, consistency and completeness.

The experimental studies of Macias *et al*. involved the thermal-neutron irradiation of palladium enriched to 93% $^{102}$Pd. Gamma spectra were studied by means of 20- and 40-cm$^3$ Ge(Li) detectors with energy resolutions FWHM ≤ 2.2 keV for 1332-keV gamma rays. A planar 0.5-cm$^3$ Ge(Li) crystal was used to quantify low-energy photon spectra, while an anti-Compton spectrometer consisting of an 8-cm$^3$ Ge(Li) diode and NaI(Tl) annulus was also employed in the gamma spectral studies. A commercial solution of $^{103}$Pd was acquired by 2021Ri01 for subsequent dilution and the preparation of six sources suitable for gamma-ray spectroscopic studies. N-type HPGe detectors were used to determine the gamma-ray emission probabilities: two 100 cm$^3$ coaxial detectors were used over the energy range 50 to 500 keV, while KX-ray and low-energy gamma-ray emissions were measured by means of a planar detector along with LX-ray studies undertaken with an additional silicon drift detector. Despite the perceived thoroughness of these two particular set of measurements by 1976Ma37 and 2021Ri01, further extensive gamma- and X-ray studies are required to improve future efforts to derive a comprehensive decay scheme with any great confidence beyond quantification of the dominant EC decay to the 39.753-keV excited state of $^{103m}$Rh and the resulting IT gamma transition to the stable ground state of $^{103}$Rh.

## Directly measured and recommended gamma-ray energies.

| $E_\gamma$ (keV) | | | | | | | | | | | |
|---|---|---|---|---|---|---|---|---|---|---|---|
| **1954Ri09** **$^{103}$Pd(EC)** | **1955Av11** **$^{103}$Pd(EC)** | **1955Sa16** **$^{103}$Ru($\beta^-$)** **$^{103}$Pd(EC)** | **1969Zo02** **$^{103}$Ru($\beta^-$)** **$^{103}$Pd(EC)** | **1969Gr13** **$^{103}$Pd(EC)** | **1969Ra18** **$^{103}$Ru($\beta^-$)** | **1970NiZV** **$^{103}$Ru($\beta^-$)** **$^{103}$Pd(EC)** | **1970Pe04** **$^{103}$Ru($\beta^-$)** | **1976Ma37** **$^{103}$Ru($\beta^-$)** **$^{103}$Pd(EC)** | **2010Kr05** **$^{103}$Ru($\beta^-$)** | **2018Ni14** **2009ENSDF** | **Weighted mean (LWM)[a]** |
| – | 40.0 (5)[b] | 40 | **39.78 (5)** | **39.748 (8)** | **39.755 (12)** | **39.75 (7)** | **39.762 (16)** | **39.73 (2)** | – | – | **39.750 ± 0.006 → 39.753 ± 0.006[c,d]** |
| – | 53? | – | **53.28 (5)** | – | **53.275 (10)** | **53.3 (9)** | **53.271 (30)** | **53.29 (1)** | **53.286 (10)** | 53.282 (7) | **53.283 ± 0.006** |
| – | 65 (1) | 65 (3) | **62.3 (2)** | **62.30 (12)** | – | **62.5 (1)** | – | **62.41 (3)** | – | – | **62.41 ± 0.03** |
| 262 (15) | – | – | **241.8 (1)** | 262? | – | – | **241.87 (25)** | **241.88 (5)** | **241.875 (10)** | – | **241.875 ± 0.010** |
| 305 (8) | 298 (2) | 300 (5) | **295.17 (10)** | **294.70 (17)** | **294.72 (12)** | **295.0 (1)** | **294.82 (8)** | **294.98 (15)** | **294.964 (10)** | 294.964 (10)[e] | **294.962 ± 0.015** |
| | ~ 330 | – | **318.0 (3)** | 330? | – | **317.4 (3)** | – | **317.72 (5)** | – | – | **317.72 ± 0.05** |
| 367 (6) | 362 (3) | 365 (5) | **357.60 (10)** | **356.98 (9)** | – | **357.5 (1)** | **357.21 (35)** | **357.45 (8)** | **357.382 (23)** | – | **357.38 ± 0.08** |
| – | – | – | 444.11 (15)[b] | – | **443.77 (12)** | **443.9 (1)** | **443.63 (12)** | **443.79 (5)** | **443.810 (10)** | 443.80 (2) | **443.809 ± 0.010** |
| 503 (8) | 498 (4) | 495 (5) | **497.23 (10)** | 496.74 (22)[b] | **497.080 (13)** | **497.1 (1)** | **496.92 (10)** | **497.08 (2)** | **497.085 (10)** | 497.083 (6) | **497.083 ± 0.007** |

[a] Weighted mean of selected gamma-ray energy measurements (no adjustments made to the weighting of the input uncertainties to give both the LWM values and uncertainties listed).
[b] Chauvenet outlier, and therefore not included in final AveTools analytical procedures to determine LWM.
[c] Single gamma transition of IT decay of $^{103m}$Rh daughter.
[d] Recommended $E_\gamma$ of 39.753 (6) keV in close agreement with $^{103m}$Rh gamma transition energy of 39.7537 (21) keV determined from $K_{ce}$ and K electron binding energy by Kovalík *et al*. (2000KoZT), and aligned exactly with $Q_{IT}$ of 39.753 (6) keV as adopted in NUBASE2020/AME2020 (2021Ko07, 2021Wa16).
[e] A value of 295.964 (10) keV was erroneously listed in Table III of 2018Ni14 – acknowledged within a direct communication from the lead author, and therefore corrected to 294.964 (10) keV (2009De29).

**Published gamma-ray emission probabilities.**

| $E_\gamma$ (keV) | $P_\gamma$ | | | | | |
|---|---|---|---|---|---|---|
| | **1954Ri09[b]** | **1955Av11[c]** | **1955Sa16[b]** | **1969Zo02[d]** | **1969Gr13[b]** | **1970NiZV[e]** |
| 39.753 ± 0.006[a] | − | 0.0021 (2) | ~ 0.1 | 211 (10) | 0.072 (6) | 1100 (90)[g] |
| 53.283 ± 0.006 | − | ≤ 0.000005[h] | − | 0.03 (1) | − | 0.23 |
| 62.41 ± 0.03 | − | 0.000040 (6) | 0.004 (1) | 2.4 (2) | 0.0042 (4) | 20 (3) |
| 241.875 ± 0.010 | 0.004 (2)[h] | − | − | − | < 0.0005[h] | − |
| 294.962 ± 0.015 | } 0.011 (3) | 0.00030 (3) | 0.012 (2) | 14.2 (14) | 0.0108 (14) | 72 (8) |
| 317.72 ± 0.05 | | ~ 0.0001 | − | 0.04 (1) | < 0.0005[h] | 0.41 (8) |
| 357.38 ± 0.08 | 0.060 (7) | 0.0021 (4) | 0.066 (10) | 100.0 | 0.0610 (30) | 531 (5) |
| 443.809 ± 0.010 | − | − | − | 0.075 (8) | − | 0.23 (6) |
| 497.083 ± 0.007 | 0.011 (2) | 0.00045 (5) | 0.01 | 17.5 (18) | 0.0140 (14) | 100 (10) |

**Published gamma-ray emission probabilities (continued).**

| $E_\gamma$ (keV) | $P_\gamma$ | | | |
|---|---|---|---|---|
| | **1976Ma37[f]** | **2002Bf07[d]** | **2004Po24[d]** | **2021Ri01[b]** |
| 39.753 ± 0.006[a] | 100 | − | – | 0.0647 (7) |
| 53.283 ± 0.006 | 0.038 (30) | − | – | < 0.000008 |
| 62.41 ± 0.03 | 1.52 (5) | − | – | 0.001128 (16) |
| 241.875 ± 0.010 | 0.0007 (7)[h] | − | − | – |
| 294.962 ± 0.015 | 4.1 (1) | 14.08 (35) | 12.3 (2) | 0.00315 (7) |
| 317.72 ± 0.05 | 0.022 (1) | − | – | 0.0000137 (17) |
| 357.38 ± 0.08 | 32.3 (10) | 100.0 (19) | 100.0 (10) | 0.02486 (17) |
| 443.809 ± 0.010 | 0.022 (1) | − | − | 0.000021 (8) |
| 497.083 ± 0.007 | 5.8 (2) | 18.15 (36) | 17.6 (3) | 0.00439 (7) |

[a] Single gamma transition of $^{103m}Rh$ daughter (IT decay).
[b] Expressed as absolute gamma-ray emission probabilities per decay (1954Ri09, 1955Sa16, 1969Gr13 - factor of 10 adjustment made to reported data of 1954Ri09), and per 100 decays (2021Ri01).
[c] Emission probabilities expressed relative to total $P_{XK}$ of 1.0.
[d] Emission probabilities expressed relative to Pγ(357.38 keV) of 100.0.
[e] Emission probabilities expressed relative to Pγ(497.81 keV) of 100 (10).
[f] Emission probabilities expressed relative to Pγ(39.753 keV) of 100.
[g] Statistical uncertainty only.
[h] Gamma emission not observed with confidence.

**Measured and recommended gamma-ray emission probabilities relative to P$_{\gamma}$(357.42 keV) of 100.**

| E$_{\gamma}$ (keV) | $P_{\gamma}^{rel}$ | | | | | |
|---|---|---|---|---|---|---|
| | **1954Ri09[a]** | **1955Av11[a]** | **1955Sa16[a]** | **1969Zo02** | **1969Gr13[a]** | **1970NiZV[a]** |
| 39.753 ± 0.006[c] | − | 100 (21) | ~ 150 | 211 (10) | 118 (12) | 207 (17)[d] |
| 53.283 ± 0.006 | − | ≤ 0.24 | − | 0.03 (1) | − | 0.04 |
| 62.41 ± 0.03 | − | 1.9 (5) | 6 (2) | 2.4 (2) | 6.9 (7) | 3.8 (6) |
| 241.875 ± 0.010 | 7 (4) | − | − | − | < 0.8 | − |
| 294.962 ± 0.015 | 18 (6) | 14 (3) | 18 (4) | 14.2 (14) | 17.7 (25) | 13.6 (15) |
| 317.72 ± 0.05 | | ~ 5 | − | 0.04 (1) | < 0.8 | 0.077 (15) |
| 357.38 ± 0.08 | 100 (16) | 100 (30) | 100 (21) | 100.0 | 100 (7) | 100 (1) |
| 443.809 ± 0.010 | − | − | − | **0.075 (8)** | − | 0.043 (11) |
| 497.083 ± 0.007 | 18 (4) | 21 (5) | 15 | **17.5 (18)** | 23 (3) | 18.8 (19) |

**Measured and recommended gamma-ray emission probabilities relative to P$_{\gamma}$(357.42 keV) of 100 (continued).**

| E$_{\gamma}$ (keV) | $P_{\gamma}^{rel}$ | | | | |
|---|---|---|---|---|---|
| | **1976Ma37[a]** | **2002Bf07** | **2004Po24** | **2021Ri01[a]** | **Recommended[b]** |
| 39.753 ± 0.006[c] | 310 (10) | − | – | **260 (3)** | **260 (3)[e]** |
| 53.283 ± 0.006 | 0.12 (9) | − | – | < 0.032 | **0.0231 (13)[f]** |
| 62.41 ± 0.03 | **4.71 (21)** | − | – | **4.54 (7)** | **4.56 (7)** |
| 241.875 ± 0.010 | 0.0022 (22) | − | – | – | **0.0032(3)[g]** |
| 294.962 ± 0.015 | **12.7 (5)** | 14.08 (35) | **12.3 (2)** | **12.7 (3)** | **12.5 (2)[h]** |
| 317.72 ± 0.05 | **0.068 (4)** | − | – | **0.055 (7)** | **0.065 (6)** |
| 357.38 ± 0.08 | **100 (4)** | **100.0 (19)** | **100.0 (10)** | **100.0 (7)** | **100.0** |
| 443.809 ± 0.010 | **0.068 (4)** | − | – | **0.08 (3)** | **0.070 (4)** |
| 497.083 ± 0.007 | **18.0 (8)** | **18.15 (36) → 18.2 (4)** | **17.6 (3)** | **17.7 (3)** | **17.8 (3)[i]** |

[a] Emission probabilities adjusted in order to be expressed relative to P$_{\gamma}$(357.38 keV) of 100 or 100.0.

[b] Apart from the highly-converted 39.753-keV γ ray and low-intensity 53.283- and 241.875-keV γ rays, weighted-mean values of the measured relative emission probabilities were adopted with uncertainties that do not fall below the most precise measurement, unless stated otherwise in the footnotes below.

[c] Single γ emission in the IT decay of daughter $^{103m}$Rh.

[d] Statistical uncertainty only.

[e] While the relative transition probability of the 39.753-keV γ ray is extremely important in defining the decay scheme with any degree of confidence, measurements of this parameter over many years have proved to be difficult and significantly disparate – a value of 260 (3) has been adopted on the basis of the recent well-defined measurement by 2021Ri01.

[f] A relative emission probability of 0.0231 (13) was adopted to achieve γ population-depopulation balance and a direct β$^{-}$ population of zero for the 93.034-keV nuclear level of $^{103}$Rh.

[g] Gamma emission not observed with confidence in the EC decay of $^{103}$Pd – tentative value of 0.0032 (3) adopted for $P_{\gamma}^{rel}$(241.875 keV) from equivalent studies of $^{103}$Ru β$^{-}$ decay of 0.0029 (3) (1976Ma37) and 0.0035 (3) (1994Sc43) involving relevant γ decays from the 536.839-kev nuclear level of $^{103}$Rh.

[h] LWM value of 12.45 (16) adjusted to 12.5 (2) to avoid the uncertainty falling below the most precise measurement.

[i] LWM value of 17.78 (18) adjusted to 17.8 (3) to avoid the uncertainty falling below the most precise measurement.

While a high fraction of the decay of $^{103}$Pd is identified with direct EC population of the 39.753-keV nuclear level of $^{103m}$Rh, a number of other higher-energy levels are also populated and undergo subsequent gamma depopulation. However, there is little to no agreement between the various sets of gamma-ray measurements that strive to quantify the lesser EC and gamma transitions. Weighted-mean analyses of the relative emission probabilities for those gamma rays with energies below 290 keV were only performed with data from 1976Ma37 and 2021Ri01, while other supportive data were taken from 1969Zo02, 2002Bf07 and 2004Po24 for gamma-ray energies above 290 keV. This whole approach can only be described as questionable, and emphasizes the need for further gamma-ray measurements.

Another feature of note is that the $^{103m}$Rh IT decay (half-life of 56.115 minutes) via a single gamma transition to the ground state of $^{103}$Rh has been included in this evaluation of the $^{103}$Pd decay scheme, with an appropriate adjustment of the emission probability of the 39.753-keV gamma ray.

Multipolarities, and Internal Conversion Coefficients

A significant number of studies have focussed on the measurement and derivation of internal conversion coefficients and mixing ratios, particularly with respect to the $^{103m}$Rh IT transition of 39.753 keV. Relevant measured and proposed data have been collected together in a series of tables displayed below, along with other related parameters such as ICC shell and subshell ratios.

**Gamma-ray emissions: proposed mixing ratios of (M1 + E2) gamma transitions.**

| $E_\gamma$ (keV) | δ | | | | |
|---|---|---|---|---|---|
| | 1977Kr13 recommended | 1981Ha11 Measured | 1981Mu18 measured | 1983Kr01 re-determined | Recommended |
| 53.28 | 0.000 (55) | − | − | − | 0.00 (5) |
| 294.96 | − 0.17 (1)[a] | − | − | − | – 0.170 (13) |
| 497.08 | − 0.125 (10) | **− 0.36 (8)**[a,b] | **− 0.42 (4)**[a] | **− 0.368 (11)**[a] | – 0.371 (35) |

[a] Used in BrIccMixing calculations to determine the recommend mixing ratio.

[b] Preferred δ value of – 0.36 (8) from gamma-ray angular distributions measurements of $\beta^-$ decay of $^{103}$Ru ground state ($3/2^+$) at temperatures down to 2.8 mK, compared with δ value of – 0.34 (5) for $\beta^-$ decay of $^{103}$Ru ground state ($5/2^+$).

The multipolarities of the gamma transitions have been defined on the basis of the known spins and parities of the relevant nuclear levels of $^{103}$Rh (2009De29), coupled with various determinations of the ICCs and subshell ratios:

39.753-keV isomeric transition of $^{103m}$Rh defined as (99.935%E3 + 0.065%M4) from a wide range of ICC and subshell ratio measurements (particularly $\alpha_K$ and $\alpha_L$ of 2018Ni14) in support of a small M4 admixture from which a mixing ratio of 0.025 (+10, –15) was adopted;

53.283-keV gamma transition assumed to be virtually 100%M1 from the ICC data of 1970Pe04 and 1976Ma37;

62.41-keV gamma transition judged to be 100%M1 from $\alpha_L$ determination by 1969Gr13 of 0.13 (4) compared with a frozen orbital approximation of 0.14;

241.875-keV gamma transition defined as pure E1 from spin and parity considerations ($5/2^+ \rightarrow 3/2^-$), and supported by $\alpha_K$ measurements of 1970Pe04 and 1976Ma37;

294.962-keV gamma transition calculated to be 97.2%M1 + 2.8%E2 from recommended δ-value of – 0.170 (13) – see also 1958Mc02, 1970RoZS, 1972Sa03 and 1977Kr13 – as supported by $\alpha_K$ measurements of 1969Gr13, 1969Ra18, 1970Pe04 and 1976Ma37;

317.72-keV gamma transition defined as pure E1 from spin and parity considerations ($5/2^- \rightarrow 7/2^+$);

357.38-keV gamma transition defined as pure E2 from spin and parity considerations ($5/2^- \rightarrow 1/2^-$), and supported by $\alpha_K$ measurements of 1969Gr13 and 1976Ma37;

443.809-keV gamma transition assumed to be pure E2 from $\alpha_K$ measurements of 1970Pe04, 1971Av03 and 1976Ma37, and spin parity considerations ($5/2^+ \rightarrow 9/2^+$);

497.083-keV gamma transition calculated to be 87.9%M1 + 12.1%E2 from recommended δ-value of – 0.371 (35) – see 1981Ha11, 1981Mu18 and 1983Kr01 – as supported by $\alpha_K$ , $\alpha_L$ and subshell ratios determined by 1952Co16, 1968Ma08, 1969Zo02, 1970Pe04, 1970NiZV, 1971Av03 and 1976Ma37.

Recommended internal conversion coefficients have been determined by means of the BrIcc code (frozen orbital approximation) of Kibédi *et al*. (2008Ki07), based on the theoretical model of Band *et al*. (2002Ba85, 2002Ra45).

**Gamma-ray emissions: measured and derived internal conversion coefficients, shell and subshell ratios, and mixing ratios.**

| $E_\gamma$ (keV) | | 1950Ko10 | 1952Co16 | 1955Av11 | 1955Dr43 | 1955Mc51 | 1958Mc02 | 1967Br04 | 1967VuZZ | 1968Ma08 | 1969Gr13[a] | 1969Le17 |
|---|---|---|---|---|---|---|---|---|---|---|---|---|
| 39.753, | $\alpha_K$ | – | – | 40 | – | – | – | – | – | – | (145) | 180 (20) |
| E3 + M4 | $\alpha_L$ | – | – | 470 | – | – | – | – | – | 1280 (260) | – | – |
| | $\alpha_M$ | – | – | – | – | – | – | – | – | – | – | – |
| | $\alpha_{total}$ | – | – | – | – | – | – | – | – | – | – | – |
| | $\alpha_K$ / $\alpha_{total}$ | – | – | – | – | – | – | – | – | – | – | – |
| | δ | – | – | – | – | – | – | – | – | – | – | – |
| | K/(K+L+M) | – | – | – | – | – | – | – | 0.099 (10)[c] | – | – | – |
| | K/L | – | 0.10 (4)[c] | 0.09 (1) | 0.18 (3) | – | – | – | – | – | – | – |
| | K/(L+M) | 0.20 (4) | – | – | – | – | – | – | – | – | – | – |
| | K/(L+M+N) | – | – | – | – | – | – | 0.0986 (50) | – | – | – | – |
| | K/(L+M+N+ …...) | – | – | – | – | – | – | – | – | – | – | – |
| | $K/L_1$ | – | – | – | – | – | – | – | – | – | 17 (6) | – |
| | $K/L_2$ | – | – | – | – | – | – | – | – | – | 0.357 (30)[c] | – |
| | $K/L_3$ | – | – | – | – | – | – | – | – | – | 0.243 (20)[c] | – |
| | K/ΣL | – | – | – | – | – | – | – | – | – | 0.143 (12)[c] | – |
| | $L_1/L_2$ | – | – | – | – | – | – | – | – | – | 0.021 (6) | – |
| | $L_1/L_3$ | – | – | – | – | – | – | – | – | – | 0.013 (4) | – |
| | $L_2/L_3$ | – | – | – | – | – | – | – | – | – | 0.682 (11)[c] | – |
| | $M_{1,2}/M_3$ | – | – | – | – | – | – | – | – | – | – | – |
| | $M_{1\text{-}3}/M_{4,5}$ | – | – | – | – | – | – | – | – | – | 33 (14) | – |
| | $M_{4,5}/M_3$ | – | – | – | – | – | – | – | – | – | – | – |
| | $M_3/L_3$ | – | – | – | – | – | – | – | – | – | – | – |
| | ΣL/ΣM | – | – | – | 7 (1) | – | – | – | – | 4.8 (7)[c] | 4.90 (13)[c,e] | – |
| | $N/M_3$ | – | – | – | – | – | – | – | – | – | – | – |
| | $NO/M_3$ | – | – | – | – | – | – | – | – | – | – | – |
| | NO/M | – | – | – | – | – | – | – | – | – | – | – |
| | ΣL/ΣN | – | – | – | – | – | – | – | – | – | 34 (3)[c] | – |
| 53.283, | $\alpha_K$ | – | – | – | – | – | – | – | – | – | – | – |
| (M1) | $\alpha_L$ | – | – | – | – | – | – | – | – | – | – | – |
| | K/L | – | – | – | – | – | – | – | – | 8.5 (9) | – | – |
| | $L_1/L_2$ | – | – | – | – | – | – | – | – | – | – | – |
| | $L_1/L_3$ | – | – | – | – | – | – | – | – | – | – | – |
| | $L_2/L_3$ | – | – | – | – | – | – | – | – | – | – | – |
| 62.41, M1 + E2 | $\alpha_L$ | – | – | – | – | – | – | – | – | – | 0.13 (4)[c] | – |
| 241.875, E1 | $\alpha_K$ | – | – | – | – | – | – | – | – | – | – | – |
| 294.962, | $\alpha_K$ | – | – | – | – | – | – | – | – | 0.024 (4) | 0.017 (8)[c] | – |
| M1 + E2 | δ | – | – | – | – | - 0.18 or - 1.17 | - 0.17 (1)[c] or - 1.2 | – | – | – | – | – |
| 357.38, E2 | $\alpha_K$ | – | – | – | – | – | – | – | – | – | 0.0121 (21)[c] | – |
| 443.809, E2 | $\alpha_K$ | – | – | – | – | – | – | – | – | 0.012 (2) | – | – |
| 497.083, | $\alpha_K$ | – | – | – | 0.0054 (10) | – | – | – | – | 0.007 (1) | 0.0029 (22) | – |
| M1 + E2 | $\alpha_L$ | – | – | – | – | – | – | – | – | – | – | – |
| | K/L | – | 8.5 (15)[c] | – | 6.0 (15) | – | – | – | – | 8.5 (7)[c] | – | – |
| | K/(L+M+ ……) | – | – | – | – | – | – | – | – | – | – | – |
| | $L_1/(L_2 + L_3)$ | – | – | – | – | – | – | – | – | – | – | – |
| | δ | – | – | – | – | – | – | – | – | – | – | – |

**Gamma-ray emissions: measured and derived internal conversion coefficients, shell and subshell ratios, and mixing ratios (continued).**

| $E_\gamma$ (keV) | | 1969Ra18 | 1969Zo02 | 1970NiZV | 1970Pe04 | 1970RoZS | 1971Av03 | 1972Br02 | 1972Pa10 | 1972Sa03 | 1974CzZY, 1975Cz03 |
|---|---|---|---|---|---|---|---|---|---|---|---|
| 39.753, E3 + M4 | $\alpha_K$ | – | – | 138 (5)[c] | 159 (25) | – | – | – | 123 (14)[c] | – | 127 (6)[c] |
| | $\alpha_L$ | – | – | – | – | – | – | – | – | – | – |
| | $\alpha_M$ | – | – | – | – | – | – | – | – | – | – |
| | $\alpha_{total}$ | – | – | – | – | – | – | – | – | – | 1531 (30)[c] |
| | $\alpha_K / \alpha_{total}$ | – | – | – | – | – | – | – | – | – | 0.0826 (50) |
| | δ | – | – | – | – | – | – | – | – | – | – |
| | K/(K+L+M) | – | – | – | – | – | – | – | – | – | – |
| | K/L | – | – | – | – | – | – | – | – | – | – |
| | K/(L+M) | – | – | – | – | – | – | – | – | – | – |
| | K/(L+M+N) | – | – | – | – | – | – | – | – | – | – |
| | K/(L+M+N+ ......) | – | – | – | – | – | – | – | – | – | 0.0914 (43) |
| | $K/L_1$ | – | – | – | – | – | – | – | – | – | – |
| | $K/L_2$ | – | – | – | – | – | – | – | – | – | – |
| | $K/L_3$ | – | – | – | – | – | – | – | – | – | – |
| | K/ΣL | – | – | – | – | – | – | – | – | – | – |
| | $L_1/L_2$ | – | – | – | 0.023 (4)[c] | – | – | – | – | – | – |
| | $L_1/L_3$ | – | – | – | 0.0163 (25) | – | – | 0.00922 (208) | – | – | – |
| | $L_2/L_3$ | – | – | – | 0.695 (6)[c] | – | – | 0.710 (15)[c] | – | – | – |
| | $M_{1,2}/M_3$ | – | – | – | – | – | – | – | – | – | – |
| | $M_{1\text{-}3}/M_{4,5}$ | – | – | – | – | – | – | – | – | – | – |
| | $M_{4,5}/M_3$ | – | – | – | – | – | – | – | – | – | – |
| | $M_3/L_3$ | – | – | – | – | – | – | – | – | – | – |
| | ΣL/ΣM | – | – | – | – | – | – | – | – | – | – |
| | $N/M_3$ | – | – | – | – | – | – | – | – | – | – |
| | $NO/M_3$ | – | – | – | – | – | – | – | – | – | – |
| | NO/M | – | – | – | – | – | – | – | – | – | – |
| | ΣL/ΣN | – | – | – | – | – | – | – | – | – | – |
| 53.283, (M1) | $\alpha_K$ | – | – | 1.77 (3) | 1.90 (19)[c] | – | 2.47 (14) | – | – | – | – |
| | $\alpha_L$ | – | – | – | – | – | – | – | – | – | – |
| | K/L | – | – | – | – | – | – | – | – | – | – |
| | $L_1/L_2$ | – | – | – | 12.1 (35) | – | – | – | – | – | – |
| | $L_1/L_3$ | – | – | – | 41 (20)[c] | – | – | – | – | – | – |
| | $L_2/L_3$ | – | – | – | 3.4 (20)[c] | – | – | – | – | – | – |
| 62.41, M1 + E2 | $\alpha_L$ | – | – | – | – | – | – | – | – | – | – |
| 241.875, E1 | $\alpha_K$ | – | – | – | 0.013 (5)[c] | – | – | – | – | – | – |
| 294.962, M1 + E2 | $\alpha_K$ | 0.016 (5)[c] | – | 0.020 (5) | 0.0176 (17)[c] | – | – | – | – | – | – |
| | δ | – | – | – | – | – 0.189 (10)[c] | – | – | – | 0.15 (1)[c] | – |
| 357.38, E2 | $\alpha_K$ | – | – | – | > 0.011 | – | – | – | – | – | – |
| 443.809, E2 | $\alpha_K$ | 0.012 (3) | – | 0.011 (3) | 0.0062 (7)[c] | – | 0.0064 (27)[c] | – | – | – | – |
| 497.083, M1 + E2 | $\alpha_K$ | 0.0058 (15) | 0.0043 (6)[c] | 0.005 (1)[c] | (0.00459) | – | 0.0044 (4)[c] | – | – | – | – |
| | $\alpha_L$ | – | – | – | – | – | – | – | – | – | – |
| | K/L | – | – | – | 8.40 (25)[c] | – | – | – | – | – | – |
| | K/(L+M+ ……) | – | – | – | – | – | 8.4 (4) | – | – | – | – |
| | $L_1/(L_2 + L_3)$ | – | – | – | 18.5 (35) | – | – | – | – | – | – |
| | δ | – | – | – | – | – | – | – | – | – | – |

**Gamma-ray emissions: measured and derived internal conversion coefficients, shell and subshell ratios, and mixing ratios (continued).**

| $E_\gamma$ (keV) | | 1975Ma32[b] | 1976Ma37 | 1977Kr13 | 1979VaZE | 1981Ha11 | 1981Mu18 | 1983Kr01 | 1999Sa78 | 2018Ni14 |
|---|---|---|---|---|---|---|---|---|---|---|
| 39.753, | $\alpha_K$ | – | 137 (19)[c] | – | 148 (18) | – | – | – | 153 (6) | 141.1 (23)[c] |
| E3 + M4 | $\alpha_L$ | – | 1014 (11) | – | – | – | – | – | 1185 (59) | – |
| | $\alpha_M$ | – | – | – | – | – | – | – | 234 (15) | – |
| | $\alpha_{total}$ | – | – | – | 1430 (89)[c] | – | – | – | – | 1428 (13)[c] |
| | $\alpha_K / \alpha_{total}$ | – | – | – | – | – | – | – | – | – |
| | δ | – | – | – | – | – | – | – | – | 0.023 (5)[c] |
| | K/(K+L+M) | – | – | – | – | – | – | – | – | – |
| | K/L | – | – | – | – | – | – | – | – | – |
| | K/(L+M) | – | – | – | – | – | – | – | – | – |
| | K/(L+M+N) | – | – | – | – | – | – | – | – | – |
| | K/(L+M+N+ …...) | – | – | – | – | – | – | – | – | – |
| | $K/L_1$ | – | – | – | – | – | – | – | – | – |
| | $K/L_2$ | – | – | – | – | – | – | – | – | – |
| | $K/L_3$ | – | – | – | – | – | – | – | – | – |
| | K/ΣL | – | – | – | – | – | – | – | – | – |
| | $L_1/L_2$ | 0.063 (12)[d] | – | – | – | – | – | – | – | – |
| | $L_1/L_3$ | 0.0432 (13)[d] | – | – | – | – | – | – | – | – |
| | $L_2/L_3$ | 0.684 (21)[c] | – | – | – | – | – | – | – | – |
| | $M_{1,2}/M_3$ | 0.76 (4)[c] | – | – | – | – | – | – | – | – |
| | $M_{1\text{-}3}/M_{4,5}$ | – | – | – | – | – | – | – | – | – |
| | $M_{4,5}/M_3$ | 0.045 (9)[c] | – | – | – | – | – | – | – | – |
| | $M_3/L_3$ | 0.215 (9)[c] | – | – | – | – | – | – | – | – |
| | ΣL/ΣM | – | – | – | – | – | – | – | – | – |
| | $N/M_3$ | 0.259 (10)[c] | – | – | – | – | – | – | – | – |
| | $NO/M_3$ | 0.274 (15)[c] | – | – | – | – | – | – | – | – |
| | NO/M | 0.150 (8)[c] | – | – | – | – | – | – | – | – |
| | ΣL/ΣN | – | – | – | – | – | – | – | – | – |
| 53.283, | $\alpha_K$ | – | 2.02 (10) and 1.74 (17) → av. 1.95 (13)[c] | – | – | – | – | – | – | – |
| (M1) | $\alpha_L$ | – | 0.18 (2)[c] | – | – | – | – | – | – | – |
| | K/L | – | – | – | – | – | – | – | – | – |
| | $L_1/L_2$ | – | – | – | – | – | – | – | – | – |
| | $L_1/L_3$ | – | – | – | – | – | – | – | – | – |
| | $L_2/L_3$ | – | – | – | – | – | – | – | – | – |
| 62.41, M1 + E2 | $\alpha_L$ | – | – | – | – | – | – | – | – | – |
| 241.875, E1 | $\alpha_K$ | – | 0.011 (3)[c] | – | – | – | – | – | – | – |
| 294.962, | $\alpha_K$ | – | 0.018 (2)[c] | – | – | – | – | – | – | – |
| M1 + E2 | δ | – | – | – 0.17 (1)[c] | – | – | – | – | – | – |
| 357.38, E2 | $\alpha_K$ | – | 0.019 (11)[c] | – | – | – | – | – | – | – |
| 443.809, E2 | $\alpha_K$ | – | 0.0069 (7)[c] | – | – | – | – | – | – | – |
| 497.083, | $\alpha_K$ | – | 0.0046 (1)[c] | – | – | – | – | – | – | – |
| M1 + E2 | $\alpha_L$ | – | 0.00055 (3)[c] | – | – | – | – | – | – | – |
| | K/L | – | 8.4 (5)[c] | – | – | – | – | – | – | – |
| | K/(L+M+ ..….) | – | – | – | – | – | – | – | – | – |
| | $L_1/(L_2 + L_3)$ | – | – | – | – | – | – | – | – | – |
| | δ | – | – | – 0.125 (10) | – | – 0.36 (8)[c] | – 0.42 (4)[c] | – 0.368 (11)[c] | – | – |

Above table - footnotes:

[a] Theoretical $\alpha_K$ value of 145 was adopted from 1968Ha52 by the authors (1969Gr13), and all other related data were normalised with respect to this particular value.

[b] Published data are experimental/theoretical ratios of the defined conversion-electron intensities – these data have been converted into their definitive experimental shell and subshell ratios in order to compare with other known measurements.

[c] Used in BrIccMixing code calculations to support recommend mixing ratios for the 39.753-, 53.283-, 294.962- and 497.083-keV gamma transitions.

[d] Doubtful value arises from the very weak ill-defined $L_1$ line.

[e] Value of 4.90 (13) calculated from the measured L and M conversion-electron intensities differs from the value of 4.39 (13) tabulated by 1969Gr13.

**Gamma multipolarities, and theoretical internal-conversion coefficients as calculated by the BrIcc code (frozen orbital approximation).**

| $E_\gamma$ (keV) | Multipolarity | $\alpha_K$ | $\alpha_L$ | $\alpha_{L1}$ | $\alpha_{L2}$ | $\alpha_{L3}$ | $\alpha_M$ | $\alpha_N$ | $\alpha_O$ | $\alpha_{total}$ |
|---|---|---|---|---|---|---|---|---|---|---|
| 39.753 (6) | 99.935%E3 + 0.065%M4<br>$\delta = 0.025^{+10}_{-15}$<br>(1950Ko10, 1952Co16, 1955Av11, 1955Dr43, 1967Br04, 1967VuZZ, 1968Ma08, 1969Gr13, 1969Le17, 1970NiZV, 1970Pe04, 1972Br02, 1972Pa10, 1975Cz03, 1975Ma32, 1976Ma37, 1979VaZE, 1999Sa78, 2018Ni14) | 142 (7) | 1051 (30) | 13 (5) | 423 (6) | 615 (18) | 214 (6) | 31.4 (9) | 0.024 (11) | 1440 (40) |
| 53.283 (6) | (M1)<br>(1968Ma08, 1970NiZV, 1970Pe04, 1971Av03, 1976Ma37) | 1.81 (3) | 0.223 (4) | 0.204 (3) | 0.01407 (20) | 0.00418 (6) | 0.0415 (6) | 0.00686 (10) | 0.000338 (5) | 2.08 (3) |
| 62.41 (3) | M1<br>(1969Gr13) | 1.143 (16) | 0.1406 (20) | 0.1294 (19) | 0.00865 (13) | 0.00258 (4) | 0.0262 (4) | 0.00433 (6) | 0.000214 (3) | 1.314 (19) |
| 241.875 (10) | E1<br>(1970Pe04, 1976Ma37) | 0.01033 (15) | 0.001202 (17) | 0.001078 (15) | 0.0000504 (7) | 0.0000734 (11) | 0.000222 (4) | 0.0000366 (6) | 0.000001761 (25) | 0.01179 (17) |
| 294.962 (15) | 97.2%M1 + 2.8%E2<br>$\delta = -0.170$ (13)<br>(1955Mc51, 1958Mc02, 1968Ma08,1969Gr13, 1969Ra18, 1970NiZV, 1970Pe04, 1970RoZS, 1972Sa03, 1976Ma37, 1977Kr13) | 0.01669 (24) | 0.00199 (3) | 0.00187 (3) | 0.0000868 (20) | 0.0000357 (18) | 0.000370 (6) | 0.0000613 (9) | 0.00000308 (5) | 0.0191 (3) |
| 317.72 (5) | E1 | 0.00493 (7) | 0.000571 (8) | 0.000521 (8) | 0.0000201 (3) | 0.0000294 (5) | 0.0001055 (15) | 0.00001741 (25) | 0.000000853 (12) | 0.00563 (8) |
| 357.38 (8) | E2<br>(1969Gr13, 1970Pe04, 1976Ma37) | 0.01368 (20) | 0.00181 (3) | 0.001434 (21) | 0.000195 (3) | 0.0001768 (25) | 0.000337 (5) | 0.0000548 (8) | 0.00000234 (4) | 0.01588 (23) |
| 443.809 (10) | E2<br>(1968Ma08, 1969Ra18, 1970NiZV, 1970Pe04, 1971Av03, 1976Ma37) | 0.00698 (10) | 0.000889 (13) | 0.000742 (11) | 0.0000790 (11) | 0.0000677 (10) | 0.0001655 (24) | 0.0000270 (4) | 0.000001215 (17) | 0.00807 (12) |
| 497.083 (7) | 87.9%M1 + 12.1%E2<br>$\delta = -0.371$ (35)<br>(1952Co16, 1955Dr43, 1968Ma08, 1969Gr13, 1969Ra18, 1969Zo02, 1970NiZV, 1970Pe04, 1971Av03, 1976Ma37, 1977Kr13, 1981Ha11, 1981Mu18, 1983Kr01) | 0.00458 (7) | 0.000539 (8) | 0.000509 (8) | 0.0000203 (8) | 0.0000100 (8) | 0.0001001 (15) | 0.00001660 (24) | 0.000000839 (12) | 0.00524 (8) |

**Parent $^{103}$Pd (half-life of 17.00 (5) d) in secular equilibrium with daughter $^{103m}$Rh (half-life of 56.115 (16) min)**

$$^{103m}Rh(t_{1/2}) < {}^{103}Pd(t_{1/2}) \rightarrow {}^{103}Pd \text{ concentration} / {}^{103m}Rh \text{ concentration} = \frac{c_{103Pd}\,(\lambda_{103mRh} - \lambda_{103Pd})}{c_{103mRh} \cdot \lambda_{103mRh}}$$

at equal detection coefficients $(c_{103Pd} = c_{103mRh})$, i.e., identical gamma-ray emission energies:

$$^{103}Pd \text{ activity}/{}^{103m}Rh \text{ activity} = \frac{(\lambda_{103mRh} - \lambda_{103Pd})}{\lambda_{103mRh}} = \frac{103Pd(t_{1/2}) - 103mRh(t_{1/2})}{103Pd(t_{1/2})}$$

$$^{103m}Rh \text{ activity}/{}^{103}Pd \text{ activity} = \frac{103Pd(t_{1/2})}{103Pd(t_{1/2}) - 103mRh(t_{1/2})} = \frac{17.00(5)}{17.00(5) - 0.038969(11)} = 1.0023\ (29)$$

## Normalisation factor – gamma rays and EC decay

EC decay directly to the ground state of $^{103}$Rh was assumed to be effectively zero on the basis of spin and parity changes that would result in a first forbidden unique transition ($5/2^+ \rightarrow 1/2^-$ (2, yes)). Therefore, the normalisation factor (*NF*) of the relative γ-ray emission probabilities can be determined on the basis of direct γ population of the ground state of $^{103}$Rh summing to 100%.

$$\sum(absolute\ \gamma\ transition\ probabilities\ direct\ to\ {}^{103}Rh\ ground\ state) = 100$$

$$\Sigma[\{P^{rel}_{slow\gamma}(39.753\ keV)\ x\ (1+\alpha_{tot})\} + \{P^{rel}_{\gamma}(294.962\ keV)\ x\ (1+\alpha_{tot})\} + \{P^{rel}_{\gamma}(357.38\ keV)\ x\ (1+\alpha_{tot})\}]\ x\ NF = 100$$

$$[(374660\ (11263)/1.0023\ (29)) + 12.74\ (20) + 101.588\ (23)]\ x\ NF = 100$$

in which the secular equilibrium of parent $^{103}$Pd and daughter $^{103m}$Rh is recognised in terms of the delayed emission of the 39.753-keV γ ray (by a factor of 1.0023 (29))

373914 (11290) x *NF* = 100

*NF* = 100 / 373915 (11290) = 0.000267 ± 0.000008

An equivalent total EC summation calculation gives an identical value: NF = 0.000267 ± 0.000008

A normalisation factor of (0.000267 ± 0.000008) was adopted in order to determine the absolute transition and emission probabilities of the EC and γ rays from their relative values.

## Transition and emission probabilities of 39.753-keV gamma ray derived from the precise decay scheme

Consider the EC and gamma population of the first excited state of $^{103}$Rh:

$$TP^{rel}_{\gamma}(39.753\ keV) = \Sigma[\{P^{abs}_{EC(0,1)} \div NF\} + \{TP^{rel}_{\gamma}(53.28\ keV)\} + \{TP^{rel}_{\gamma}(317.72\ keV)\} + \{TP^{rel}_{\gamma}(497.98\ keV)\}]$$

= $\Sigma$[{99.9646 (9) ÷ 0.000267 (8)} + 0.071 (4) + 0.065 (6) + 17.9 (3)] = [374399 (11218) + 18.0 (3)] = 374417 (11218)

$TP^{abs}_{\gamma}(39.753\ keV)$ = 374417 (11218) x 0.000267 (8) = 100 (4)% from above,

and 99.9695 (12)%, if overall accuracy is aligned with the determination of $P^{abs}_{EC(0,1)}(534.9\ keV)$;
also adjustments to $P^{rel}_{\gamma}(39.753\ keV)$ = 260 (11) → 260 (3),
and $P^{abs}_{\gamma}(39.753\ keV)$ = 0.069375 (1926)% → 0.0694 (19)%.

**Recommended gamma-ray energies, and relative and absolute emission probabilities and transition probabilities of 100% EC decay of $^{103}$Pd/$^{103m}$Rh.**

| | E$_\gamma$ (keV) | $P^{rel}_{\gamma}$ | $TP^{rel}_{\gamma}$ | $P^{abs}_{\gamma}$ (%)[a] | Absolute transition probability (%) |
|---|---|---|---|---|---|
| $\gamma_{1,0}$ | 39.753 (6) | 260 (3) | 374417 (11218) | 0.069375 (1926) → 0.0694 (19)[a] | 100 (4) → 99.9695 (12)[b] |
| $\gamma_{2,1}$ | 53.283 (6) | 0.0231 (13) | 0.071 (4) | 0.0000062 (4) | 0.0000190 (12) |
| $\gamma_{4,3}$ | 62.41 (3) | 4.56 (7) | 10.55 (18) | 0.00122 (4) | 0.00282 (10) |
| $\gamma_{5,3}$ | 241.875 (10) | 0.0032 (3) | 0.0032 (3) | 0.00000085 (8) | 0.00000086 (8) |
| $\gamma_{3,0}$ | 294.962 (15) | 12.5 (2) | 12.74 (20) | 0.00334 (11)[a] | 0.00340 (11) |
| $\gamma_{4,1}$ | 317.72 (5) | 0.065 (6) | 0.065 (6) | 0.0000174 (17) | 0.0000175 (17) |
| $\gamma_{4,0}$ | 357.38 (8) | 100.0 | 101.588 (23) | 0.0267 (8)[a] | 0.0271 (8) |
| $\gamma_{5,2}$ | 443.809 (10) | 0.070 (4) | 0.071 (4) | 0.0000187 (12) | 0.0000189 (12) |
| $\gamma_{5,1}$ | 497.083 (7) | 17.8 (3) | 17.9 (3) | 0.00475 (16) | 0.00477 (16) |

[a] Uncertainties of $P^{abs}_{\gamma}$ for three γ emissions that populate the ground state directly and sum to 100% in terms of their transition probabilities were assessed by means of the GABS code, version 12, 20 June 2021 to avoid double accounting of uncertainties (39.753-, 294.96- and 357.38-keV) → $P^{abs}_{\gamma}(39.753\ keV)$ re-defined as 0.0694 (19)% rather than 0.069 (22)%, whereas there is no equivalent impact on the uncertainties of $P^{abs}_{\gamma}$(294.96- and 357.38-keV).

[b] $TP^{abs}_{\gamma}$ adjusted from 100 (4) on the basis of summed total TP$_\gamma$ ground-state population of 100%, with contributions of 0.00340 (11)% and 0.0271 (8)% from the 294.96- and 357.38-keV γ transitions, respectively, to give a very precise TP$_\gamma$(39.753 keV) of 99.9695 (12)%.

The GABS code was used to convert the evaluated relative γ-ray emission probabilities to absolute values per 100 decays of the $^{103}$Pd parent nucleus, along with their uncertainties (GABS, version 12, 20 June 2021, ENSDF analysis program). Gamma rays that directly populate the nuclear levels involved in the calculation of the normalisation factor were identified prior to these calculations in order to avoid double accounting of their uncertainties during the course of this process.

Electron energies were determined from electron binding energies tabulated by Larkins (1977La19) and the evaluated gamma-ray energies. Absolute electron emission probabilities were calculated from the evaluated absolute gamma-ray emission probabilities and associated internal conversion coefficients.

**Energies and emission probabilities of noteworthy internal conversion electrons from 100% EC decay of $^{103}$Pd/$^{103m}$Rh.**

| | | Energy (keV) | Electrons per 100 disint. |
|---|---|---|---|
| $ec_{1,0\ T}$ | (Rh) | 16.533 – 39.751 | 99.9695 (12) |
| $ec_{1,0\ K}$ | (Rh) | 16.533 (6) | 9.9 (6) |
| $ec_{1,0\ L}$ | (Rh) | 36.341 – 36.749 | 73 (3) |
| $ec_{1,0\ M}$ | (Rh) | 39.126 – 39.446 | 14.9 (6) |
| $ec_{1,0\ N+}$ | (Rh) | 39.672 – 39.751 | 2.2 (1) |

The relatively simple decay scheme of $^{103}$Pd is completely dominated by the EC transition which populates the 39.753-keV metastable state of $^{103}$Rh with an absolute EC transition probability of 99.9646%. As a consequence, all other gamma transitions possess low to extremely low absolute transition probabilities, apart from the 39.753-keV gamma decay from $^{103m}$Rh to the stable ground state of $^{103}$Rh. Under such circumstances, there is also no evidence of reasonable agreement between the seven sets of experimental studies in which Ge(Li) detectors of good resolution were used to measure the gamma-ray emission probabilities (1969Zo02, 1969Gr13, 1970NiZV, 1976Ma37, 2002Bf07, 2004Po24 and 2021Ri01). Despite some misgivings, the more extensive measurements of 1976Ma37 and 2021Ri01 were most regularly accepted in this evaluation along with other more limited γ-ray emission data to be found within 1969Zo02, 2002Bf07 and 2004Po24. Furthermore, a relative $P_\gamma$(53.283 keV) of 0.0231 (13) was calculated by achieving a balanced gamma population-depopulation of the 93.031-keV nuclear level of $^{103}$Rh, while a tentative value of 0.0032 (3) was adopted for the relative $P_\gamma$(241.85 keV) on the basis of equivalent $\beta^-$ decay studies of $^{103}$Ru (1976Ma37, 1994Sc43). Although the assumption that no EC transition populates the $^{103}$Rh ground state directly is questionable, the transition probability has been judged to be sufficiently low as to assign a value of zero, while direct EC decay to the 93.031-keV nuclear level of $^{103}$Rh was similarly defined as zero from spin-parity considerations.

## EC Transitions

Energies

The recommended nuclear level energies and evaluated $Q_{EC}$-value of 574.7 (24) keV for the $^{103}$Pd ground-state to $^{103}$Rh ground-state transition were used to determine the recommended energies and uncertainties of the EC transitions (2021Wa16).

Transition Probabilities

EC transition probabilities were derived for the population-depopulation imbalances of the relative emission probabilities of the gamma rays and their theoretical internal-conversion, and a normalisation factor of 0.000267 ± 0.000008 for the gamma-ray emissions as calculated above. EC decay directly to both the 93.031-keV nuclear level and ground state of $^{103}$Rh were assumed to be effectively zero on the basis of spin and parity considerations that would result in second forbidden non-unique and first forbidden unique transitions, respectively. The BetaShape code was adopted to calculate the log*ft* and fractional EC probabilities $P_K$, $P_L$, $P_M$ and $P_N$, as defined and developed further from the data tabulations of 1995ScZY and 1998Sc28 (BetaShape code, version 2.3.1, December 2023, LNHB analysis program (2015Mo10, 2019Mo35, 2023Mo21)).

**Recommended EC decay of $^{103}$Pd as derived by means of the BetaShape code (2015Mo10, 2019Mo35, 2023Mo21).**

| | $E_{EC}$ (keV)[a] | $P_{EC}$ (%) | $^{103}$Pd | $^{103}$Rh | transition type | log *ft* | $P_K$ | $P_L$ | $P_{L1}$ | $P_{L2}$ |
|---|---|---|---|---|---|---|---|---|---|---|
| $EC_{0,5}$ | 37.9 (24) | 0.00480 (16) | 5/2 + | 5/2 + | allowed | 7.33 (11) | 0.55 (5) | 0.35 (4) | 0.34 (4) | 0.0065 (7) |
| $EC_{0,4}$ | 217.3 (24) | 0.0300 (9) | 5/2 + | 5/2 − | first forbidden non-unique | 8.569 (18) | 0.8459 (6) | 0.1226 (4) | 0.1204 (4) | 0.002255 (8) |
| $EC_{0,3}$ | 279.7 (24) | 0.00058 (7) | 5/2 + | 3/2 − | first forbidden non-unique | 10.52 (5) | 0.8518 (5) | 0.11804 (26) | 0.11587 (25) | 0.002171 (6) |
| $EC_{0,2}$ | 481.7 (24) | zero | 5/2 + | 9/2 + | [second forbidden non-unique] | − | − | − | − | − |
| $EC_{0,1}$ | 534.9 (24) | 99.9646 (9) | 5/2 + | 7/2 + | allowed | 5.880 (6) | 0.86086 (30) | 0.11103 (15) | 0.10899 (15) | 0.002047 (4) |
| $EC_{0,0}$ | 574.7 (24) | zero | 5/2 + | 1/2 − | [first forbidden unique] | − | − | − | − | − |
| | | Σ 100.0000 (13) | | | | | | | | |

[a] Determined from the recommended nuclear level energies and Q-value of 574.7 (24) keV (2021Wa16).

| | $E_{EC}$ (keV)[a] | $P_M$ | $P_N$ |
|---|---|---|---|
| $EC_{0,5}$ | 37.9 (24) | 0.084 (11) | 0.0186 (25) |
| $EC_{0,4}$ | 217.3 (24) | 0.02589 (17) | 0.00563 (6) |
| $EC_{0,3}$ | 279.7 (24) | 0.02479 (14) | 0.00538 (5) |
| $EC_{0,2}$ | 481.7 (24) | – | – |
| $EC_{0,1}$ | 534.9 (24) | 0.02310 (11) | 0.00501 (4) |
| $EC_{0,0}$ | 574.7 (24) | – | – |

A consistent decay scheme was derived that consists of four EC transitions and nine gamma-ray emissions (with the 39.753-keV gamma decay of $^{103m}$Rh included in the existing data set), of which almost all of the EC decay is directly to the 39.753-keV metastable state of $^{103}$Rh ((99.9646 ± 0.0009)%).

## Atomic Data

Measurements of the total KX-ray emission probability and Auger-electron emission probabilities have been carried out, and are listed below for $^{103}$Ru as well as $^{103}$Pd and $^{103m}$Rh. The X-ray related data of direct applicability to the $^{103}$Pd-$^{103m}$Rh system has been assessed more thoroughly in terms of the measurements of $P_{KX}$, $P_{K\alpha}/P_{K\beta}$ and $P_\gamma$(357.42 keV)/$P_{KX}$. As listed in the table below, the experimental studies of the KX emission probabilities associated with $^{103}$Pd EC decay exhibit reasonable agreement (1976Ma37, 1978Ne09, 2002Bf07, 2021Ri01), and compare well with the BrIccEmis/NS_RadList calculation for $P_{KXtotal}$ of 77.5%. Furthermore, the measured KX emission probabilities for the 39.753-keV gamma transition of $^{103m}$Rh are in good agreement (1967Br04, 1967VuZZ, 1969Gr13, 1973In07, 1974Sa15, 1975Cz03, 1981Va22, 1994Sc43, 2018Ri01), and are well aligned with the BrIccEmis/NS_RadList calculation of 8.1 (4)% for $P_{KXtotal}$ (see DDEP file for fully separated $^{103m}$Rh decay data).

The absolute emission probabilities of both the KX-ray and 357.42-keV γ ray have been used to determine cross-section data for the production of $^{103}$Pd from Rh targets (2009Ta10). Recommended decay data were adopted from the ENSDF evaluation of De Frenne and Jacobs (2001De37), and a difference of the order of 25% was observed between the activities obtained by means of these particular recommended X- and γ-ray photopeaks. The mass chain for A = 103 was re-evaluated in 2009 for ENSDF (2009De29):

$$P_{KX} = 76.9\ (14);\ \ P_\gamma(357\text{ keV}) = 0.0221\ (7) \ \rightarrow\ P_\gamma(357\text{ keV})/P_{KX} \text{ ratio of } 0.000287\ (11)$$

Decay-data measurements by Berlyand *et al*. (2002Bf07) furnished emission probabilities for the $K_\alpha$ and $K_\beta$ X-rays relative to the 357.42-keV γ ray to give a value of 0.000369 (11) for the $P_\gamma$(357 keV)/$P_{KX}$ ratio, compared with the value of 0.000287 adopted and used previously (ENSDF 2002).

Effectively, the current evaluation of the $^{103}$Pd decay scheme results in a recommended $P_\gamma$(357.42 keV) of 0.0267 (8)% and $P_{KXtotal}$ of 77.5 (4)% to produce a $P_\gamma$(357 keV)/$P_{KX}$ ratio of 0.000345 (11), and the latter value is comparable with LWM and NRM weighted-mean averages of 0.000335 (15) and 0.000349 (8), respectively, that are based upon the measurements of 1976Ma37, 1978Ne09, 2002Bf07 and 2021Ri01.

**KX-ray emission probability per 100 disintegrations and X-γ emission ratios of $^{103m}$Rh, $^{103}$Ru/$^{103m}$Rh and $^{103}$Pd/$^{103m}$Rh decay.**

| Reference | $P_{KX}$ (%) | $P_{K\alpha}/P_{K\beta}$ | $P_\gamma$(357 keV)/$P_{KX}$ | Target processing (if any) and detector systems |
|---|---|---|---|---|
| **1967Br04**<br>**$^{103}$Ru/$^{103m}$Rh** | 7.00 (35) | – | – | Neutron irradiation of Ru metal to produce $^{103}$Ru – purification two months after irradiation → fusion with KOH/$KNO_3$ to form perruthenate for dissolution in $H_2SO_4$ solution, followed by rapid $RuO_4$ distillation. Study of five $^{103}$Ru/$^{103m}$Rh sources in equilibrium.<br>measured growth of 20-keV X-ray – two NaI(Tl) crystal detectors; absolute $^{103}$Ru activity – 4πβ-γ counting and NaI(Tl) γ detector. |
| **1967VuZZ**<br>**$^{103m}$Rh** | 7.7 (8) | – | – | Neutron irradiation of metallic Rh foils ($^{103}$Rh(n,n') $^{103m}$Rh).<br>4π$K_{ce}$–KX-ray coincidence technique, no earlier than 1.5 hours after irradiation – 4π proportional counter and thin NaI crystal detector. |
| **1969Gr13**<br>**$^{103}$Pd/$^{103m}$Rh** | 8.4 (8)[a] | – | 0.00085 (7)<br><br>$P_\gamma$(39.753 keV)/$P_{KX}$ = 0.0086 (11) | $^{103}$Pd extracted radiochemically from deuteron- and proton-irradiated Rh metallic plate and powder targets – difficult dissolution in hot $H_2SO_4$ solution, then Pd activity extracted by means of dimethyl-glyoxime-chelate in chloroform, and electroplated on to Cu foils.<br>Also neutron-irradiation of 96%-enriched metallic $^{102}$Pd target (in the form of strips deposited on Al-foil backing) to produce $^{103}$Pd sources.<br>electron spectra – double-focussing iron-yoke β spectrometer;<br>γ and X-rays – Ge(Li) detector and NaI(Tl) crystal. |
| **1969Le17**<br>**$^{103}$Pd/$^{103m}$Rh**<br>**$^{103m}$Rh** | –<br>– | 5.0 (2) Pd fraction;<br>4.7 (2) Rh fraction | –<br>– | Proton irradiation of Rh foil to produce $^{103}$Pd, which was dissolved electrolytically in HCl and diluted, prior to separation of Pd(II) in organic layer from Rh(III) in aqueous layer by addition of dithizone in chloroform.<br>X-rays – NaI(Tl) and Ge(Li) detectors. |
| **1973In07**<br>**$^{103}$Ru/$^{103m}$Rh**<br>**$^{103m}$Rh** | 7.03 (44) | – | – | Thermal-neutron irradiation of Ru metal to produce $^{103}$Ru –purification five weeks after irradiation → metal target dissolved in NaClO prior to electrodeposition on Au foil.<br>measurement and attenuation of KX-rays and 39.753-keV γ ray – thin NaI(Tl) cleaved crystal;<br>γ rays and γ-KX-ray coincidence – Ge(Li) detector;<br>attenuation of Rh X-rays emitted by $^{102}$Rh source;<br>absolute detection efficiency of thick Rh source ($^{102}$Rh). |
| **1974Sa15**<br>**$^{103m}$Rh** | 6.97 (28) | – | – | Variable-energy neutron irradiation of Rh metal (with a range of thickness) sandwiched between discs of pressed sulphur → thin $^{103m}$Rh sources prepared after chemical separation from any resulting $^{103}$Ru activity.<br>X-rays and 4πce-X-ray coincidence – NaI(Tl) crystal. |
| **1975Cz03**<br>**$^{103m}$Rh** | 6.76 (5)[b] | – | – | $^{103m}$Rh source prepared by elution from $^{103}$Pd-$^{103m}$Rh generator.<br>γ rays, X-rays and 4πce-X-ray coincidence counting – NaI(Tl) crystal. |
| **1976Ma37**<br>**$^{103}$Ru/$^{103m}$Rh**<br>**$^{103}$Pd/$^{103m}$Rh** | 80 (5) | – | **<u>0.000299 (9)</u>**<br><br>$P_\gamma$(39.753keV)/$P_{KX}$ = 0.00093 | Thermal-neutron irradiation of Ru powder (enriched to 99% weight % 102) to produce $^{103}$Ru, and Pd metal (enriched to 93% in mass 102) to produce $^{103}$Pd → all sources purified radiochemically and deposited ($^{103}$Ru) or electroplated ($^{103}$Pd) on to suitable backing foils.<br>20- and 40-$cm^3$ Ge(Li) detectors;<br>planar 0.5-$cm^3$ Ge(Li) detector for low-energy photons;<br>8-$cm^3$ Ge(Li) anti-Compton detector with NaI(Tl) annulus to give a photopeak-to-Compton ratio of 200:1 for 1332-keV of $^{60}$Co. |
| **1978Ne09**<br>**$^{103}$Pd/$^{103m}$Rh** | – | – | **<u>0.000307 (10)</u>**[c] | Harwell: $^{103}$Pd solution evaporated and deposited on to a paper filter.<br>"phoswich" detector system – NaI(Tl) detector for X-rays; 40-$cm^3$ coaxial Ge(Li) detector for γ rays.<br>Livermore: $^{103}PdCl_2$ flashed from a hot tungsten filament on to aluminised Mylar film.<br>Si(Li) and Ge(Li) detectors for X- and γ rays. |
| **1981Va22**<br>**$^{103m}$Rh** | 8.44 (9)[d] | – | **–** | $^{103m}$Rh source prepared by elution from $^{103}$Pd-$^{103m}$Rh generator by means of anion exchange columns.<br>activity measurements – liquid scintillation counter;<br>KX-rays – two Si(Li) detectors. |

| Reference | $P_{KX}$ (%) | $P_{K\alpha}/P_{K\beta}$ | $P_\gamma$(357 keV)/$P_{KX}$ | Target processing (if any) and detector systems |
|---|---|---|---|---|
| **1994Sc43** **$^{103}$Ru/$^{103m}$Rh** | 8.54 (11) | 4.81 (10) | – <br> $P_\gamma$(39.753 keV)/$P_{KX}$ = 0.0083 (3) | Four sources of dried droplets of a $^{103}$Ru solution were used to study $^{103}$Ru-$^{103m}$Rh decay. <br> activity measurements – well-type ionization chamber for 4πβ-γ coincidence counting; <br> Si(Li) and HPGe detectors for X- and γ rays. |
| **2002Bf07** **$^{103}$Pd/$^{103m}$Rh** | 61.2 (23) | 5.05 (18) | **0.000369 (11)** | Seven weightless $^{103}$Pd sources from an OSGI standard. <br> X-ray spectroscopy – OChG detector, <br> γ-ray spectroscopy – 40- and 80-cm$^3$ Ge(Li) detectors. |
| **2004Po24** **$^{103}$Pd/$^{103m}$Rh** | – | 5.1 (4) | – | Neutron-irradiation of Pd (enriched to 99.5% weight % $^{102}$Pd) for 18 days, followed by radiochemical extraction of $^{103}$Pd from the irradiated target to prepare 1-ml sources of $HNO_3$-based solutions. Data expressed at a confidence level of 0.95 (2σ). <br> three HPGe detectors with energy resolutions of ~ 0.6, ~ 3.0 and ~ 3.2 keV for 661.7-keV γ ray of $^{137}$Cs; <br> HPGe detector with energy resolution of ~ 0.5 keV for 24-keV $K_\alpha$ X-ray of Sn. |
| **2018Ri01** **$^{103m}$Rh** | 8.25 (17) | 5.07 (17) | – <br> $P_\gamma$(39.753 keV)/$P_{KX}$ = 0.0096 (5) | Neutron-irradiation of both a pure compacted $^{103}$Rh metallic powder pellet and $RhCl_3$ powder target, followed by post-irradiation decay of short-lived $^{104,104m}$Rh. Samples processed and measured in parallel: (1) X-rays → compacted $^{103}$Rh pellet, and five aqueous $RhCl_3$ sources after target dissolution in small volume of water), and (2) TDCR liquid scintillation counter (five sources after dissolution of $^{103}$Rh pellet, and the five existing sources of $RhCl_3$). $XK_\alpha$ = 6.89 (17)%; $XK_\beta$ = 1.36 (3)%; $XK_{total}$ = 8.25 (17)%; $P_\gamma$(39.75 keV) = 0.079 (4)%. Gamma-ray impurities within the sources were also assessed and quantified by means of a large coaxial HPGe detector. <br> absolute activity – liquid scintillation counter (triple-to-double coincidence ratio method); <br> X-rays – low-energy planar HPGe detector. |
| **2021Ri01** **$^{103}$Pd/$^{103m}$Rh** | 71.1 (6) | 4.90 (6) | **0.000350 (4)** <br> $P_\gamma$(39.753keV)/$P_{KX}$ = 0.000910 (13) | $^{103}$Pd supplied by NORDION in 2019 ($PdCl_3$ in dilute $NH_4OH$, and stabilized subsequently by addition of HCl). Six point sources prepared by means of deposition and drying on Mylar sheets sealed with a thin foil for γ-ray spectroscopy, and six sources of ~ 20-fold dilution for liquid scintillation counting; $P_\gamma$(357 keV)/$P_{KX}$ uncertainty of ± 0.000004 adjusted to ± 0.000006 to reduce weighting from 0.6712 to 0.50 in the LWM calculations. <br> mass activity – TDCR liquid scintillation counter, <br> γ-ray spectroscopy – two 100-cm$^3$ coaxial HPGe detectors for 50 to 500 keV γ rays; <br> planar HPGE detector for low-energy γ and X-rays; <br> silicon drift detector (SDD) for L X-rays. |
| **mean value** | – | – | **0.000335 (15) LWM** <br> **0.000349 (8) NRM** | $\chi^2/(N-1)$ = 13.43; $\chi^2/(N-1)_{cric}$ = 3.78 at 99% confidence <br> $\chi^2/(N-1)$ = 4.39; $\chi^2/(N-1)_{cric}$ = 2.60 at 95% confidence |

[a] Obtained by multiplying measurement of K-shell conversion-electron emission probability by 1969Gr13 of 10.4 (9) with K-shell fluorescence yield (0.807 (31), 1972Bb16).

[b] Quantified in the abstract, but not mentioned within the main text of the paper (1975Cz03).

[c] Weighted mean of three measurements coupled with an uncertainty aligned with the smallest uncertainty involved in the calculation of the average value (0.000331 (22) – Harwell, UK; 0.000316 (25) – Harwell, UK; 0.000301 (10) – Livermore, USA).

[d] Weighted mean of five measurements coupled with an uncertainty aligned with the smallest uncertainty involved in the calculation of the average value (8.20 (21), 8.40 (21), 8.47 (11), 8.54 (12), 8.42 (9)).

**Measured Auger-electron intensities and intensity ratios identified with $^{103}$Pd-$^{103m}$Rh decay.**

| $P_{Ae}$ | 1955Av11[a] | 1969Gr13[b] (%) | 2000KoZQ | 2000KoZS (%) |
|---|---|---|---|---|
| **KLL** | 0.27 (2) | 12.3 (11) | – | – |
| **KLX** | 0.10 (1) | 5.2 (7) | – | – |
| **KXY** | – | 0.56 (25) | – | – |
| **$KL_1L_2(^3P_0)/(^1P_1)$ ratio** | – | – | 0.21 (3) | – |
| **$KL_1L_1(^1S_0)$** | – | – | – | 10.4 (4) |
| **$KL_1L_2(^1P_1)$** | – | – | – | 13.3 (3) |
| **$KL_1L_2(^3P_0)$** | – | – | – | 2.9 (3) |
| **$KL_1L_3(^3P_1)$** | – | – | – | 9.0 (4) |
| **$KL_1L_3(^3P_2)$** | – | – | – | 2.0 (4) |
| **$KL_2L_2(^1S_0)$** | – | – | – | 3.2 (3) |
| **$KL_2L_3(^1D_2)$** | – | – | – | 43.2 (9) |
| **$KL_3L_3(^3P_0)$** | – | – | – | 2.0 (4) |
| **$KL_3L_3(^3P_2)$** | – | – | – | 14.0 (5) |

[a] Emission probabilities expressed relative to total 37-keV L conversion-electron emission of 1.0.
[b] Emission probabilities expressed as percentage of total decay.

Further measurements of the X- and γ-ray emission probabilities are highly desirable to assist in resolving the current difficulties in the proposed decay scheme that create significant anomalies of the order of 25% in the derivation of $^{103}$Pd production cross sections. This disparity is most likely to occur as a consequence of the difficulty in quantifying both the KX-ray and low-energy γ-ray emissions to the necessary precision, particularly the important but rather ill-defined $P_\gamma$(39.753 keV) – the value of this specific parameter impacts significantly on the γ-ray normalisation factor, all resulting absolute γ-ray emission probabilities, and component $P_{KX}$ data. These relatively low-energy photon emissions need to be quantified with confidence and good accuracy in order to calculate excitation functions, and so ensure the optimum production and purity of $^{103}$Pd-$^{103m}$Rh with confidence.

X-ray decay data for $^{103}$Pd/$^{103m}$Rh have been measured experimentally over many years, and most recently by Riffaud *et al.* (2021Ri01). Both X-ray and Auger-electron data have been calculated on the basis of the evaluated gamma-ray data, along with atomic data from 1996Sc06, 1998ScZM, 1999ScZX and 2000Sc47 (Rh: $\omega_K$ = 0.809 (4); $\varpi_L$ = 0.0494 (12); $n_{KL}$ = 0.987 (4)). Both the X-ray and Auger-electron spectra for the EC decay of $^{103}$Pd/$^{103m}$Rh have been calculated by means of the BrIccEmis code within NS-RadList, as described in 2012Le09, 2013LeZX, 2016Le19, 2020TeZY and 2023Texx in order to achieve the necessary detail and resolution of these spectral lines. A vacancy reaching the valence shell is immediately filled by an electron from the surrounding condensed-phase material to generate more atomic radiation, and this process will terminate when all such vacancies are filled below the valence shell. Transition energies within each propagation step were derived from the atomic binding energies determined by means of the relativistic Dirac-Fock approach employed in the RAINE code (2002Ba85), along with the application of a semi-empirical correction procedure that aligns these energies more fully with known spectral data (2020TeZY). Fixed transition rates were obtained from the EADL database (1991PeZY, 1993Cu08). Resulting X-ray energies and emission probabilities are listed below for $^{103}$Pd, followed by the recommended Auger-electron energies and emission probabilities (both sets of energies are listed as mean energies and as a range of energies at the 95% confidence level, with additional extensions of these energy ranges in italicsfor specific of X-ray and Auger electron emissions). The number of simulated nuclear events is $10^6$, and the intensity cut-off for these listings is 0.01 per 100 decays. Quoted uncertainties include direct contributions from only electron capture and internal-conversion electrons (2023Texx) – these data do not include significant uncertainties from the more complex but less well-defined atomic radiation probabilities as considered semi-quantitatively in EADL (1991PeZY). As defined by 1991PeZY, uncertainties in these theoretical X-ray emission probabilities are ~ 10% for the K and L shells and can be of the order of 30% and more for the outer shells, whereas uncertainties in the theoretical Auger-electron emission probabilities are < 15% for the K and L shells (except for Coster-Kronig and super Coster-Kronig transitions) and of the order of 30% and more for the Coster-Kronig and super Coster-Kronig transitions and the outer shells.

**X-ray energies and emission probabilities of $^{103}$Pd/$^{103m}$Rh (BrIccEmis/NS_RadList).**

| | | Mean Energy (keV) | Energy (keV) 95% confidence range/extension | Photons per 100 decays[a] |
|---|---|---|---|---|
| $X_{tot}$ | (Rh) | 18.640 | 2.703 – 22.725 | 87.0 (4) |
| $XK_{tot}$ | (Rh) | 20.599 | 20.073 – 23.167/*23.173* | 77.5 (4) |
| XKL2 | (Rh) | 20.073 | 20.073 | 22.36 (11) |
| XKL3 | (Rh) | 20.215 | 20.215 | 42.39 (20) |
| XKM | (Rh) | 22.717 | 22.699 – 22.725 | 10.68 (5) |
| XKM2 | (Rh) | 22.699 | 22.699 | 3.606 (17) |
| XKM3 | (Rh) | 22.725 | 22.725 | 7.021 (33) |
| XKN | (Rh) | 23.171 | 23.167 – 23.173 | 2.104 (10) |
| XKN2 | (Rh) | 23.167 | 23.167 | 0.7169 (34) |
| XKN3 | (Rh) | 23.173 | 23.173 | 1.383 (7) |
| $XL_{tot}$ | (Rh) | 2.747 | 2.378 – 3.094 | 9.24 (10) |
| $XM_{tot}$ | (Rh) | 0.324 | 0.188 – 0.553 | 0.2595 (23) |
| $XN_{tot}$ | (Rh) | 0.048 | 0.029 – 0.063 | 0.02001 (14) |

[a] Quoted uncertainties include direct contributions from only electron capture and internal-conversion electrons (2023Texx) – these data do not include significant uncertainties from the more complex but less well-defined atomic radiation probabilities as considered semi-quantitatively in EADL, whereby uncertainties in the theoretical X-ray radiative rates are ~ 10% for the K and L shells, and can be of the order of 30% for the outer shells (1991PeZY).

**Auger-electron energies and emission probabilities of $^{103}$Pd/$^{103m}$Rh (BrIccEmis/NS_RadList).**

| | | Mean Energy (keV) | Energy (keV) 95% confidence range/extension | Electrons per 100 decays[a] |
|---|---|---|---|---|
| Auger total | (Rh) | 0.650 | 0.002 – 2.632 | 1283 (12) |
| Auger $K_{tot}$ | (Rh) | 17.708 | 16.281 – 21.922/*22.838* | 18.42 (9) |
| Auger KLL | (Rh) | 16.811 | 16.281 – 17.083 | 12.90 (6) |
| Auger KLX | (Rh) | 19.574 | 19.133 – 20.146 | 5.043 (24) |
| Auger KXY | (Rh) | 22.275 | 21.922 – 22.838 | 0.4760 (23) |
| Auger $L_{tot}$ | (Rh) | 2.027 | *0.004*/0.044 – 2.768/*3.260* | 195.0 (20) |
| Auger Coster-Kronig LLM | (Rh) | 0.040 | 0.004 – 0.051 | 10.41 (+22-17) |
| Auger Coster-Kronig LLX | (Rh) | 0.142 | 0.031 – 0.385 | 13.68 (15) |
| Auger LMM | (Rh) | 2.236 | 1.842 – 2.490 | 143.1 (15) |
| Auger LMX | (Rh) | 2.603 | 2.370 – 2.824 | 26.45 (28) |
| Auger LXY | (Rh) | 2.977 | 2.851 – 3.260 | 1.339 (14) |
| Auger $M_{tot}$ | (Rh) | 0.198 | *0.016*/0.041 – 0.369/*0.394* | 514 (5) |
| Auger Coster-Kronig MMX | (Rh) | 0.097 | 0.016 – 0.178 | 149.5 (13) |
| Auger MXY | (Rh) | 0.239 | 0.140 – 0.394 | 364.6 (35) |
| Auger $N_{tot}$ | (Rh) | 0.019 | 0.001 – 0.034/*0.058* | 555 (5) |
| Auger super Coster-Kronig NNN | (Rh) | 0.019 | 0.001 – 0.034 | 525 (5) |
| Auger Coster-Kronig NNX | (Rh) | 0.018 | 0.002 – 0.058 | 30.46 (21) |

[a] Quoted uncertainties include direct contributions from only electron capture and internal-conversion electrons (2023Texx) – these data do not include significant uncertainties from the more complex but less well-defined atomic radiation probabilities as considered semi-quantitatively in EADL, whereby uncertainties in the theoretical Auger-electron radiative rates are < 15% for the K and L shells (except for Coster-Kronig and super Coster-Kronig transitions), and can be of the order of 30% or more for Coster-Kronig and super Coster-Kronig transitions and the outer shells (1991PeZY).

Total energy release per decay as determined from the BrIccEmis/NS_RadList studies:

| Radiation | Total energy (keV per decay) | Total intensity (%) |
|---|---|---|
| Neutrinos | 514.8 (21) | – |
| Gamma rays | 0.157 (3) | 0.1055 (33) |
| Conversion electrons | 35.2 (+12-11) | 100 (+4-3) |
| Auger electrons | 8.32 (8) | 1283 (12) |
| X-rays | 16.21 (8) | 87.1 (4) |
| Total | 574.7 (25) | |

The final X-ray and Auger-electron spectra were effectively evaluated from one million simulated nuclear decay events. Both component spectra of the Auger-electron and X-ray emissions as calculated by the BrIccEmis code for the EC decay of $^{103}$Pd are shown in the following figure.

**Auger-electron (upper panel) and X-ray (lower panel) spectra of $^{103}$Pd EC decay:**

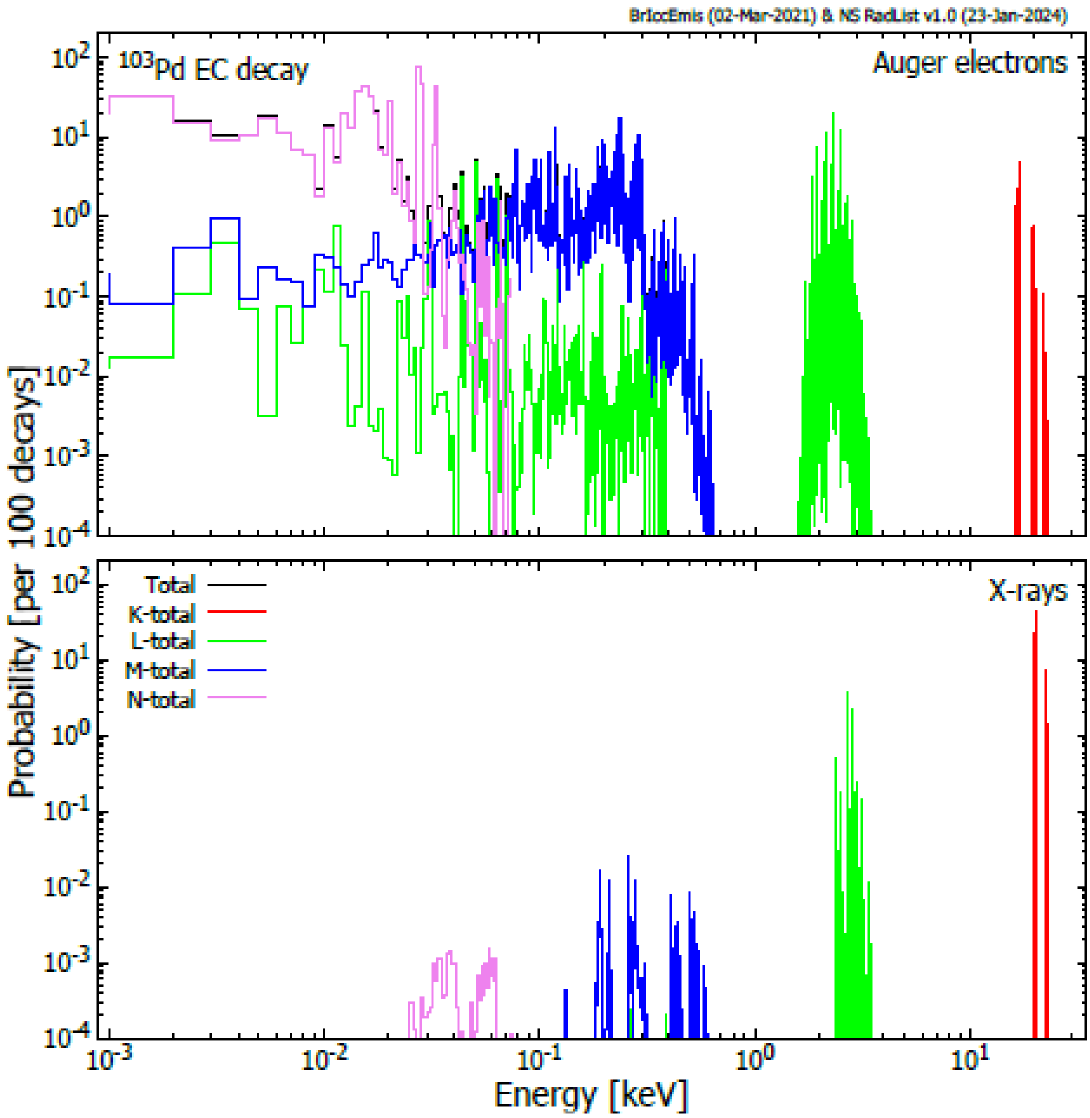


The IT decay of $^{103m}$Rh has been included as part of the decay scheme of $^{103}$Pd in this particular evaluation, as well as treated separately elsewhere to produce an entirely independent file. Auger-electron data have also been calculated by means of the BrIccEmis code to aid in both the generation and resolution of extensive spectral lines for confident application in microdosimetry.

## Main Production Modes for $^{103}$Pd

| | | | | |
|---|---|---|---|---|
| $^{103}$Pd: | $^{102}$Pd(n,γ)$^{103}$Pd, | $^{nat}$Pd(n,xn)$^{103}$Pd, | $^{103}$Rh(p,n)$^{103}$Pd, | $^{107}$Ag(p,αn)$^{103}$Pd, |
| | $^{102}$Pd(d,p)$^{103}$Pd, | $^{103}$Rh(d,2n)$^{103}$Pd, | $^{107}$Ag(d,α2n)$^{103}$Pd, | $^{103}$Rh(α,p3n)$^{103}$Pd, |
| | $^{nat}$Ag(p,2pxn)$^{103}$Pd, | $^{nat}$In(p,4pxn)$^{103}$Pd | | |

## Data Consistency

### $^{103}$Pd/$^{103m}$Rh

A $Q_{EC}$-value of 534.9 (24) keV to the metastable excited state of $^{103m}$Rh has been adopted from the atomic mass evaluation 2020 of Wang *et al*. (2021Wa16), and $Q_{IT}$-value of 39.753 (6) keV for $^{103m}$Rh IT decay to the ground state of $^{103}$Rh have been adopted from NUBASE2020 as formulated by Kondev *et al*. (2021Ko07) while in the course of defining the decay scheme of $^{103}$Pd. These data total to a $Q_{EC}$-value of 574.7 (24) keV when defined in terms of a $^{103}$Pd ground-state to $^{103}$Rh ground-state decay, which has been compared with the Q-value calculated by summing the contributions of the individual emissions to the $^{103}$Pd EC-decay and $^{103m}$Rh IT-decay processes (i.e., EC, electron, γ, etc.):

calculated Q-value = $\sum (E_i \times P_i)$ = 574.7 (25) keV

Percentage deviation from the Q-value of Wang *et al*. is (0.0 ± 0.6)%, which supports the derivation of a consistent decay scheme with a modest variant.

## References


1944Fl01 A. Flammersfeld, Kernanregung durch Schnelle Neutronen bei Rhodium und Silber, Naturwissenschaften **32** (1944) 36-37. [$^{103m}$Rh half-life]

1945Wi03 M.L. Wiedenbeck, The Nuclear Excitation of Krypton and Rhodium, Phys. Rev. **68** (1945) 237-239. [$^{103m}$Rh half-life]

1945Wi12 M.L. Wiedenbeck, The Nuclear Excitation of Rhodium, Phys. Rev. **67** (1945) 267-268. [$^{103m}$Rh half-life]

1947Fl03 A. Flammersfeld, O. Bruna, Die Anregungsenergie der Isomeren Zustände des Rhodiums 103 und 104, Z. Naturforsch. **2a** (1947) 241-244. [$^{103m}$Rh half-life]

1947Ma32 D.E. Matthews, M.L. Pool, X-ray Emission from Radioactive Ce, Pd and Ca, Phys. Rev. **72** (1947) 163-164, G8. [$^{103}$Pd half-life]

1948Li03 M. Lindner, I. Perlman, Neutron Deficient Isotopes of Rhodium and Palladium, Phys. Rev. **73** (1948) 1202-1203. [$^{103}$Pd half-life]

1950Ko10 E. Kondaiah, Disintegration of $Ru^{103}$, Phys. Rev. **79** (1950) 891-892. [K/(L+M) ratio (40 keV)]

1950Me26 J.Y. Mei, C.M. Huddleston, A.C.G. Mitchell, The Disintegration of Ruthenium-103 and Palladium-103, Phys. Rev. **79** (1950) 429-432. [$^{103m}$Rh half-life]

1952Co16 J.M. Cork, J.M. LeBlanc, F.B. Stumpf, W.H. Nestor, The Radioactive Decay of Ruthenium 103, Phys. Rev. **86** (1952) 575-576. [K/L ratios]

1953Me24 W.W. Meinke, Half-life of $Pd^{109}$ and Neutron Activation Cross Section of $Pd^{102}$, Phys. Rev. **90** (1953) 410-412. [$^{103}$Pd half-life]

1954Ri09 L.H.Th. Rietjens, H.J. Van Den Bold, P.M. Endt, Continuous and Discrete Gamma-radiation in the Decay of $^{103}$Pd, Physica **20** (1954) 107-114. [$^{103}$Pd half-life, $E_γ$, $P_γ$]

1955Av11 P. Avignon, A. Michalowicz, R. Bouchez, Étude de la Désintégration du $^{103}$Pd, J. Phys. Radium **16** (1955) 404-410. [$E_γ$, $P_γ$, $α_K$, $α_L$, K/L ratio]

1955Dr43 G.M. Drabkin, V.I. Orlov, L.I. Rusinov, Investigation of the Nuclear Isomerism of $Zn^{69}$, $Se^{79}$, $Se^{81}$, $Rh^{103}$ and $Ba^{137}$, Izvest. Akad. Nauk SSSR, Ser. Fiz., Columbia Tech. Transl. **19** (1956) 294-304. [$α_K$, K/L and L/M ratios]

1955Mc51 F.K. McGowan, P.H. Stelson, Angular Distribution of Gamma Rays from Coulomb Excitation, Phys. Rev. **99** (1955) 127-134. [δ (295 keV)]

1955Sa16 B. Saraf, Energy Levels of $Rh^{103}$ from the Decay of $Pd^{103}$ and $Ru^{103}$, Phys. Rev. **97** (1955) 715-720. [$E_γ$, $P_γ$]

1957Jo19 G.A. Jones, W.R. Phillips, Electrical Octupole Coulomb Excitation in Rhodium, Proc. Royal Soc. (London) **239A** (1957) 487-493. [$^{103m}$Rh half-life]

1958Mc02 F.K. McGowan, P.H. Stelson, Yields, Angular Distributions, and Polarization of Gamma Rays from Coulomb Excitation, Phys. Rev. **109** (1958) 901-916. [δ (295 keV)]

1967Br04 A.M. Bresesti, M. Bresesti, H. Neumann, Measurement of K X-ray Emission in the Decay of $^{103m}$Rh, J. Inorg. Nucl. Chem. **29** (1967) 15-20.
[$^{103}$Ru $\beta^-$ decay: $P_{KX}$, K/(L+M+N) ratio of 39.75-keV gamma transition]

1967VuZZ A. Vuorinen, Calibration of $^{103m}$Rh by the Coincidence Method, pp. 257-263, Proc. Symp. Standardization of Radionuclides, IAEA, Vienna, Austria (1967).
[$^{103m}$Rh half-life, K/(K + L + M) ratio, $P_{KX}$ of 39.75-keV gamma transition]

1968Ha52 R.S. Hager, E.C. Seltzer, Internal Conversion Tables, Part 1: K-, L-, M-shell Conversion Coefficients for Z = 30 to Z = 103, Nucl. Data **A4** (1968) 1-235. [Theoretical ICC]

1968Ma08 J.C. Manthuruthil, H.J. Hennecke, C.R. Cothern, Internal-Conversion-Electron Study of the Decay of Ru$^{103}$, Phys. Rev. **165** (1968) 1363-1370. [ICC, multipolarities, mixing ratios]

1968Pa24 J.A. Panontin, N.T. Porile, A.A. Caretto, Jr., Nuclear Reactions of Silver and Indium with 200- and 400-MeV Protons, Phys. Rev. **165** (1968) 1273-1281. [$^{103}$Pd half-life]

1969Gr13 Y. Grunditz, S. Antman, H. Pettersson, M. Saraceno, Studies in the Decay of $^{103}$Pd, Nucl. Phys. **A133** (1969) 369-384.
[$^{103}$Pd half-life, $E_\gamma$, $P_\gamma$, $\alpha_K$, subshell ratios, $P_{KX}$ and P(357 keV)/$P_{KX}$ ratio of $^{103}$Pd-$^{103m}$Rh]

1969KoZW Y. Kobayashi, Half-lives of Rhodium-106, -105 and -103m, JAERI report JAERI-1178 (1969) 21-22. [$^{103m}$Rh half-life]

1969Le17 M.A. Lepri, W.S. Lyon, Decay of $^{103}$Pd–$^{103m}$Rh, Int. J. Appl. Radiat. Isot. **20** (1969) 297-298.
[$K_\alpha/K_\beta$ $^{103}$Pd-$^{103}$Rh, 39.75-keV $\alpha_K$]

1969Ra18 D.E. Raeside, J.J. Reidy, M.L. Wiedenbeck, The Levels of $^{103}$Rh Populated in the Decay of $^{103}$Ru, Nucl. Phys. **A134** (1969) 347-352. [$E_\gamma$, $\alpha_K$]

1969Zo02 W.H. Zoller, E.S. Macias, M.B. Perkal, W.B. Walters, Decay of 40 d $^{103}$Ru and 17 d $^{103}$Pd to Levels of $^{103}$Rh, Nucl. Phys. **A130** (1969) 293-304. [$E_\gamma$, $P_\gamma$, $\alpha_K$(497 keV), γ-γ]

1970NiZV E.B. Nieschmidt, D.A. Pearson, Nuclear Levels of $^{103}$Rh, IN-1317 (1970) 122-126.
[$E_\gamma$, $P_\gamma$, $\alpha_K$, L subshell ratios]

1970Pe04 H. Pettersson, S. Antman, Y. Grunditz, Studies in the Decay of $^{103}$Ru, Z. Phys. **233** (1970) 260-274; Erratum, Z. Phys. **235** (1970) 485. [$E_\gamma$, $L_1/L_2$, $L_1/L_3$, $L_2/L_3$ ratios, $\alpha_K$]

1970RoZS W.M. Roney, H.W. Kugel, G.M. Heestand, R.R. Borchers, R. Kalish, Magnetic Moments of Core Excited States of Odd Nuclei Near A = 100, pp. 419-423 in Proc. Int. Conf. Nuclear Reactions Induced by Heavy Ions, 15-18 July 1969, Heidelberg, Germany, Editors: R. Bock, W.R. Hering, North-Holland Pub. Corp., Amsterdam (1970). [δ (295 keV)]

1971Av03 F.T. Avignone III, G.D. Frey, Internal-conversion and γ–γ Directional-correlation Studies in the Decay of $^{103}$Ru, Phys. Rev. **C4** (1971) 912-918. [$\alpha_K$, K/(L+M+ ….) ratio, multipolarity]

1972Bb16 W. Bambynek, B. Crasemann, R.W. Fink, H.-U. Freund, H. Mark, C.D. Swift, R.E. Price, P. Venugopala Rao, X-Ray Fluorescence Yields, Auger, and Coster-Kronig Transition Probabilities, Rev. Mod. Phys. **44** (1972) 716-813; Erratum, Rev. Mod. Phys. **46** (1974) 853. [K-shell fluorescence yield]

1972Br02 D.S. Brenner, M.L. Perlman, Subshell Conversion-line Intensity Ratios for Some Pure Transitions, Nucl. Phys. **A181** (1972) 207-216. [39.75-keV $L_1/L_3$, $L_2/L_3$ ratios]

1972Ja01 H.C. Jain, S.K. Bhattacherjee, C.V.K. Baba, Half-lives of 9/2$^+$ Levels in Some Odd-mass Rh and Ag Nuclei, Nucl. Phys. **A178** (1972) 437-448. [93-keV level half-life of $^{103}$Rh]

1972Pa10 A. Pazsit, J. Csikai, Cross Sections of the Reactions In$^{113}$(n,n')In$^{113m}$ and Rh$^{103}$(n,n')Rh$^{103m}$, Sov. J. Nucl. Phys. **35** (1972) 232-233. [$^{103m}$Rh half-life, $\alpha_K$(39.75 keV)]

1972Sa03 R.O. Sayer, J.K. Temperley, D. Eccleshell, Negative Parity Levels in $^{103}$Rh via Coulomb Excitation, Nucl. Phys. **A179** (1972) 122-140. [δ (295 keV)]

1973Ba32 Chr. Bargholtz, J. Becker, L. Eriksson, L. Gidefeldt, L. Holmberg, V. Stefánsson, Gamma-gamma Directional Correlations in $^{103}$Rh, Phys. Scr. **8** (1973) 90-94. [93-keV level half-life of $^{103}$Rh]

1973Gu06 E. Günther, K. Knauf, K.F. Walz, The Half-life of $^{103m}$Rh, Int. J. Appl. Radiat. Isot. **24** (1973) 87-89. [$^{103m}$Rh half-life]

1973In07 H. Ing, W.G. Cross, Absolute Counting of K X-rays from $^{103m}$Rh in Thick Foils, Int. J. Appl. Radiat. Isot. **24** (1973) 437-450. [$^{103}$Ru $\beta^-$ decay: $P_{KX}$ of $^{103}$Ru-$^{103m}$Rh]

1974CzZY K.H. Czock, N. Haselberger, F. Reichel, The Disintegration of $^{103m}$Rh, IAEA report IAEA/RL/26 (1974). [$\alpha_{total}$, $\alpha_K$, K/(L + M + …..) ratio]

1974Sa15 D.C. Santry, J.P. Butler, Cross Section Measurements for the $^{103}$Rh(n,n') $^{103m}$Rh Reaction from 0.122 to 14.74 MeV, Can. J. Phys. **52** (1974) 1421-1428. [$^{103m}$Rh half-life, $P_{KX}$ of $^{103m}$Rh]

1975Cz03 K.H. Czock, N. Haselberger, F. Reichel, The Disintegration of $^{103m}$Rh, Int. J. Appl. Radiat. Isot. **26** (1975) 417-421. [$\alpha_{total}$, $\alpha_K$, $P_{KX}$ of $^{103m}$Rh]

1975Cz05 K.H. Czock, N. Haselberger, F. Reichel, S. Popa, Determination of the Half-life of $^{103}$Pd, Int. J. Appl. Radiat. Isot. **26** (1975) 782-784. [$^{103}$Pd half-life]

1975Ma32 B. Martin, D. Merkert, J.L. Campbell, Intensity Ratios of L, M, N, O Subshell Conversion Electrons in M3 and E4 Transitions, Z. Phys. **A274** (1975) 15-21. [39.75-keV $L_1/L_2$, $L_1/L_3$, $L_2/L_3$, M, N, O ratios]

1976Ma37 E.S. Macias, M.E. Phelps, D.G. Sarantites, R.A. Meyer, Decay of 39-day $^{103}$Ru and 17-day $^{103}$Pd to the Levels of $^{103}$Rh, Phys. Rev. **C14** (1976) 639-644. [$E_\gamma$, $P_\gamma$, $\alpha_K$, $\alpha_L$, $P_{KX}$ and P(357 keV)/$P_{KX}$ ratio of $^{103}$Pd-$^{103m}$Rh]

1977Kr13 K.S. Krane, E2, M1 Multipole Mixing Ratios in Odd-mass Nuclei 59 ≤ A ≤ 149, At. Data Nucl. Data Tables **19** (1977) 363-416. [δ]

1977La19 F.P. Larkins, Semiempirical Auger-electron Energies for Elements 10 ≤ Z ≤ 100, At. Data Nucl. Data Tables **20** (1977) 311-387. [Auger-electron energies]

1978La21 F. Lagoutine, J. Legrand, C. Bac, Périodes de Quelques Radionucléides, Int. J. Appl. Radiat. Isot. **29** (1978) 269-272. [$^{103m}$Rh half-life]

1978Ne09 D. Newton, A.E.R. Toureau, A.L. Anderson, R.A. Meyer, Relative High-energy Gamma- and X-ray Emissions Following the Decay of $^{103}$Pd, Int. J. Appl. Radiat. Isot. **29** (1978) 188-189. [$E_\gamma$, $P_\gamma$, P(357 keV)/$P_{KX}$ ratio of $^{103}$Pd-$^{103m}$Rh]

1979VaZE R. Vaninbroukx, G. Grosse, W. Zehner, Studies of the Decay of $^{103m}$Rh, NEA report NEANDC(E)-202U, Vol. III (1979) 28-30. [$P_\gamma$, $P_{KX}$, $\alpha_{total}$, $\alpha_K$ of $^{103m}$Rh]

1981Ha11 E. Hagn, J. Wese, G. Eska, Nuclear Orientation Study of $^{97,103,105}$Ru in Fe, Z. Phys. – Atoms and Nuclei **A299** (1981) 353-358. [497.1-keV δ]

1981Mu18 D.W. Murray, A.L. Allsop, N.J. Stone, The Magnetic Moment of $^{103}$Ru, Hyperfine Interactions **11** (1981) 127-139. [497.1-keV δ]

1981Va11 R. Vaninbroukx, G. Grosse, W. Zehner, New Determinations of the Half-lives of $^{57}$Co, $^{103}$Ru, $^{103m}$Rh, $^{103}$Pd and $^{109}$Cd, Int. J. Appl. Radiat. Isot. **32** (1981) 589-591. [$^{103}$Pd and $^{103m}$Rh half-lives]

1981Va22 R. Vaninbroukx, W. Zehner, Determination of the K X-ray Emission Probability in the Decay of $^{103m}$Rh, Int. J. Appl. Radiat. Isot. **32** (1981) 850. [$^{103m}$Rh $P_{KX}$]

1983Kr01 K.S. Krane, Nuclear orientation of $^{103}$Ru: Re-analysis, Phys. Rev. **C27** (1983) 411-412. [497.1-keV δ]

1991PeZY S.T. Perkins, D.E. Cullen, M.H. Chen, J.H. Hubbell, J. Rathkopf, J. Scofield, Tables and Graphs of Atomic Subshell and Relaxation Data Derived from the LLNL Evaluated Atomic Data Library (EADL), Z = 1–100, Lawrence Livermore National Laboratory report UCRL-50400, **30** (1991). [atomic database]

1993Cu08 D.E. Cullen, S.T. Perkins, S.M. Seltzer, Photon and Electron Databases and Their Use in Radiation Transport Calculations, Appl. Radiat. Isot. **44** (1993) 1343-1347. [atomic database]

1994Sc43 U. Schötzig, Photon Emission Probabilities in the Decay of $^{103}$Ru/$^{103m}$Rh, Appl. Radiat. Isot. **45** (1994) 641-644. [$^{103m}$Rh $P_{KX}$]

1995ScZY E. Schönfeld, Tables for the Calculation of Electron Capture Probabilities, PTB Report PTB-6.33-95-2, 1995. [$P_K$, $P_L$, $P_M$, $P_N$, $P_O$]

1996Sc06 E. Schönfeld, H. Janβen, Evaluation of Atomic Shell Data, Nucl. Instrum. Methods Phys. Res. **A369** (1996) 527-533. [$\omega_K$, $\varpi_L$, $K_\beta/K_\alpha$, $K_{\alpha2}/K_{\alpha1}$, KLX/KLL, KXY/KLL]

1998Sc28 E. Schönfeld, Calculation of Fractional Electron Capture Probabilities, Appl. Radiat. Isot. **49** (1998) 1353-1357. [$P_K$, $P_L$, $P_M$, $P_N$, $P_O$]

1998ScZM E. Schönfeld, G. Rodloff, Tables of the Energies of K-Auger Electrons for Elements with Atomic Numbers in the Range from Z = 11 to Z = 100, PTB Report PTB-6.11-98-1, October 1998. [Auger electrons]

1999Sa78 M. Sainath, K. Venkataramaniah, Measurement of $\alpha_K$, $\alpha_L$, $\alpha_M$ of the Hindered E3 Transition in $^{103}$Rh, Indian J. Pure Appl. Phys. **37** (1999) 87-91. [39.75-keV $\alpha_K$, $\alpha_L$, $\alpha_M$]

1999ScZX E. Schönfeld, G. Rodloff, Energies and Relative Emission Probabilities of K X-rays for Elements with Atomic Numbers in the Range from Z = 5 to Z = 100, PTB Report PTB-6.11-1999-1, February 1999. [$X_K$]

2000KoZQ A. Kovalík, E.A. Yakushev, D.V. Filosofov, A.F. Novgorodov, V.M. Gorozhankin, I. Štekl, P. Petev, M.A. Mahmoud, The Predicted Strong Influence of the Relativistic Effects on the $KL_1L_2(^3P_0)$ Auger Transition Rate Proved for Z = 32, 45, 59 and 61, Program and Thesis, Proc. 50th Ann. Conf. Nucl. Spectrosc. Struct. At. Nuclei, St. Petersburg, Russia (2000) 178. [$^{103}$Rh $KL_1L_2$ Auger spectrum]

2000KoZS A. Kovalík, A.F. Novgorodov, E.A. Yakushev, V.M. Gorozhankin, P. Petev, M.A. Mahmoud, The KLL Auger Spectrum of $^{103}_{45}Rh$ from the EC Decay of $^{103}_{46}Pd$, Program and Thesis, Proc. 50th Ann. Conf. Nucl. Spectrosc. Struct. At. Nuclei, St. Petersburg, Russia (2000) 176. [$^{103}$Rh KLL Auger spectrum]

2000KoZT A. Kovalík, E.A. Yakushev, D.V. Filosofov, V.M. Gorozhankin, V.G. Kalinnikov, Energies of the 39.7 keV E3 Transition in $^{103}$Rh, the 25.6 keV E1 Transition in $^{161}$Dy, the 74.6 keV and 76.2 keV M1 Transitions in $^{161}$Ho, and 67.2 keV E3 and 71.9 keV M1 + E2 Transitions in $^{158}$Ho, Program and Thesis, Proc. 50th Ann. Conf. Nucl. Spectrosc. Struct. At. Nuclei, St. Petersburg, Russia (2000) 175. [39.7537(21)-keV γ-ray energy $^{103m}$Rh]

2000Sc47 E. Schönfeld, H. Janβen, Calculation of Emission Probabilities of X-rays and Auger Electrons Emitted in Radioactive Disintegration Processes, Appl. Radiat. Isot. **52** (2000) 595-600. [$P_X$, $P_{Ae}$]

2001De37 D. De Frenne, E. Jacobs, Nuclear Data Sheets for A = 103, Nucl. Data Sheets **93** (2001) 447-598. [Nuclear levels]

2002Ba85 I.M. Band, M.B. Trzhaskovskaya, C.W. Nestor, Jr., P.O. Tikkanen, S. Raman, Dirac–Fock Internal Conversion Coefficients, At. Data Nucl. Data Tables **81** (2002) 1-334. [Theoretical ICC]

2002Bf07 T.P. Berlyand, E.I. Grigor'ev, V.P. Orlov, Measurement of the Relative Intensity of $^{103}$Pd Photon Radiation, Measurement Techniques **45** (2002) 974-977. [$^{103}$Pd EC decay: $P_\gamma$, $P_X$, $K_\alpha/K_\beta$, P(357 keV)/$P_{KX}$ ratio of $^{103}$Pd-$^{103m}$Rh]

2002Ra45 S. Raman, C.W. Nestor, Jr., A. Ichihara, M.B. Trzhaskovskaya, How Good are the Internal Conversion Coefficients Now? Phys. Rev. **C66** (2002) 044312, 1-23. [Theoretical ICC]

2004Po24 Yu.S. Popov, L.V. Zakharova, V.N. Kupriyanov, O.I. Andreev, A.N. Pakhomov, F.Z. Vakhetov, Half-life and Photon Intensities of $^{103}$Pd, Radiochemistry **46** (2004) 209-210. [$^{103}$Pd half-life, $P_\gamma$, $P_X$, $K_\alpha/K_\beta$]

2008Ki07 T. Kibédi, T.W. Burrows, M.B. Trzhaskovskaya, P.M. Davidson, C.W. Nestor, Jr., Evaluation of Theoretical Conversion Coefficients using BrIcc, Nucl. Instrum. Methods Phys. Res. **A589** (2008) 202-229. [Theoretical ICC]

2009De29 D. De Frenne, Nuclear Data Sheets for A = 103, Nucl. Data Sheets **110** (2009) 2081-2256. [Nuclear levels]

2009Ta10 F. Tárkányi, A. Hermanne, B. Király, S. Takács, F. Ditrói, J. Csikai, A. Fenyvesi, M.S. Uddin, M. Hagiwara, M. Baba, T. Ido, Yu.N. Shubin, A.V. Ignatyuk, New Cross Sections for Production of $^{103}$Pd – Review of Charged-particle Production Routes, Appl. Radiat. Isot. **67** (2009) 1574-1581. [Discrepancies in $P_\gamma$ and $P_{KX}$]

2010Kr05 K.S. Krane, Neutron Capture by Ru: Neutron Cross Sections of $^{96,102,104}$Ru and γ-ray Spectroscopy in the Decays of $^{97,103,105}$Ru, Phys. Rev. **C81** (2010) 044310, 1-10. [$E_\gamma$, $^{103}$Rh nuclear level energies]

2012Le09 B.Q. Lee, T. Kibédi, A.E. Stuchbery, K.A. Robertson, Atomic Radiations in the Decay of Medical Radioisotopes – A Physics Perspective, Comput. Math. Methods Med. Article ID 651475 (2012) 1-14, doi:10.1155/2012/651475. [Atomic radiation]

2013LeZX B.Q. Lee, T. Kibédi, A.E. Stuchbery, K.A. Robertson, F.G. Kondev, A Model to Realize the Potential of Auger Electrons for Radiotherapy, Proc. Heavy Ion Accelerator Symposium (HIAS2013), 8-12 April 2013, Canberra, Australia, EPJ Web of Conferences, **63** (2013) 01002, 1-5, editors: C. Simenel, M. Evers, T. Kibédi, D. Huy Luong, M. Reed, M. Srncik, A. Wallner; doi.org/10.1051/epjconf/20136301002. [Auger electrons]

2015Mo10 X. Mougeot, Reliability of Usual Assumptions in the Calculation of β and ν Spectra, Phys. Rev. **C91** (2015) 055504, 1-12; Erratum, Phys. Rev. **C92** (2015) 059902, 1. [β decay (BetaShape code)]

2016Le19 B.Q. Lee, Hooshang Nikjoo, J. Ekman, P. Jönsson, A.E. Stuchbery, T. Kibédi, A Stochastic Cascade Model for Auger-electron Emitting Radionuclides, Int. J. Radiat. Biol. **92** (2016) 641-653; doi: 10.3109/09553002.2016.1153810. [Atomic radiation]

2018Ni14 N. Nica, J.C. Hardy, V.E. Iacob, V. Horvat, H.I. Park, T.A. Werke, K.J. Glennon, C.M. Folden III, V.I. Sabla, J.B. Bryant, X.K. James, M.B. Trzhaskovskaya, Precise Measurement of $\alpha_K$ and $\alpha_T$ for the 39.8-keV E3 transition in $^{103}$Rh: Test of Internal-conversion Theory, Phys. Rev. **C98** (2018) 054321, 1-11. [$\alpha_K$, $\alpha_T$, $\delta$ (39.75-keV $\gamma$-ray transition)]

2018Ri01 J. Riffaud, P. Cassette, D. Lacour, V. Lourenço, I. Tartès, M.A. Kellett, M. Corbel, M.-C. Lépy, C. Domergue, C. Destouches, H. Carcreff, O. Vigneau, Measurement of Absolute K X-ray Emission Intensities in the Decay of $^{103m}$Rh, Appl. Radiat. Isot. **134** (2018) 399-405. [$^{103m}$Rh IT decay: absolute $P_{KX}$, absolute $P_\gamma$]

2019Mo35 X. Mougeot, Towards High-precision Calculation of Electron Capture Decays, Appl. Radiat. Isot. **154** (2019) 108884, 1-8. [EC/$\beta^+$ decay (BetaShape code)]

2020TeZY B.P.E. Tee, T. Kibédi, B.Q. Lee, M. Vos, R. du Rietz, A.E. Stuchbery, Development of a New Database for Auger-electron and X-ray Spectra, Proc. Heavy Ion Accelerator Symposium (HIAS2019), 9-13 September 2019, Canberra, Australia, EPJ Web of Conferences, **232** (2020) 01006, 1-4, editors: A.J. Mitchell, S. Pavetich, D. Koll; doi.org/10.1051/epjconf/202023201006. [Atomic radiation]

2021Ko07 F.G. Kondev, Meng Wang, W.J. Huang, S. Naimi, G. Audi, The NUBASE2020 Evaluation of Nuclear Physics Properties, Chin. Phys. **C45** (2021) 030001, 1-180; doi: 10.1088/1674-1137/abddae [$Q_{IT}$($^{103m}$Rh)]

2021Ri01 J. Riffaud, M.-C. Lépy, P. Cassette, M. Corbel, M.A. Kellett, V. Lourenço, Measurement of the Absolute Gamma-ray Emission Intensities from the Decay of $^{103}$Pd, Appl. Radiat. Isot. **167** (2021) 109298, 1-9. [$^{103}$Pd half-life, absolute $P_{KX}$, relative $P_{LX}$, absolute $P_\gamma$]

2021Wa16 Meng Wang, W.J. Huang, F.G. Kondev, G. Audi, S. Naimi, The AME2020 Atomic Mass Evaluation (II): Tables, Graphs and References, Chin. Phys. **C45** (2021) 030003, 1-512; doi: 10.1088/1674-1137/abddaf [Q-values]

2023Mo21 X. Mougeot, Atomic Exchange Correction in Forbidden Unique Beta Transitions, Appl. Radiat. Isot. **201** (2023) 111018, 1-6. [$\beta$ decay (BetaShape code)]

2023Texx B.P.E. Tee, T. Kibédi, B.Q. Lee, A.E. Stuchbery, BrIccEmisDB Database and Computational Tool to Evaluate Atomic Relaxation Radiations, in preparation for submission to At. Data Nucl. Data Tables (2023-2024). [Atomic radiation]

90 references and three errata – 93 items

**ENSDF Analysis Programs:**
GTOL, version 7.2h, 24 May 2013
GABS, version 12, 20 June 2021
BrIcc, version 2.3b, 16 December 2014
BrIccEmis, 2 March 2021
NS_RadList, version 1.0, 7 December 2023
BrIccMixing, version 2.3d, 28 September 2019

**ENSDF Utility Programs:**
Avetools, version 3.0, 11 December 2014
V.AveLib, version 06-22, 19 March 2024

FMTCHK, version 10.4d, 7 September 2022

**LNHB Analysis Program**
BetaShape, version 2.3.1, December 2023

The above codes have undergone and will continue to undergo various forms of modification and improvement, which will be reflected in changes to the version number and date of issue into the public domain. Assistance from Xavier Mougeot (LNHB, CEA Saclay, France – BetaShape) and Tibor Kibédi (ANU, Australia – particularly BrIccEmis) concerning improved operational features of some of the above codes is gratefully acknowledged by ALN.